Solar Energy 264 (2023) 111998

Contents lists available at ScienceDirect

Solar Energy

journal homepage: www.elsevier.com/locate/solener

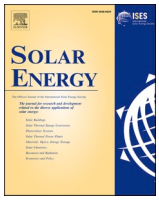

Review

State-of-the-art in solar water heating (SWH) systems for sustainable solar energy utilization: A comprehensive review

Md. Rashid Al-Mamun [a,b,1], Hridoy Roy [c,1], Md. Shahinoor Islam [c,d,*], Md. Romzan Ali [a], Md. Ikram Hossain [a], Mohamed Aly Saad Aly [e], Md. Zaved Hossain Khan [a,*], Hadi M. Marwani [f,g], Aminul Islam [h], Enamul Haque [i], Mohammed M. Rahman [f,g], Md. Rabiul Awual [j,k,l,*]

[a] Department of Chemical Engineering, Jashore University of Science and Technology, Jashore 7408, Bangladesh
[b] Department of Civil and Environmental Engineering, University of Alberta, Edmonton T6G 1H9, Alberta, Canada
[c] Department of Chemical Engineering, Bangladesh University of Engineering and Technology, Dhaka-1000, Bangladesh
[d] Department of Textile Engineering, Daffodil International University, Dhaka 1341, Bangladesh
[e] Department of Electrical and Computer Engineering(ECE), Georgia Tech Shenzhen Institute (GTSI), Tianjin University, Guangdong 518055, China
[f] Center of Excellence for Advanced Materials Research, King Abdulaziz University, Jeddah 21589, Saudi Arabia
[g] Chemistry Department, Faculty of Science, King Abdulaziz University, Jeddah 21589, Saudi Arabia
[h] Department of Petroleum and Mining Engineering, Jashore University of Science and Technology, Jashore-7408, Bangladesh
[i] School of Engineering, RMIT University, Melbourne, Victoria 3000, Australia
[j] Materials Science and Research Center, Japan Atomic Energy Agency (JAEA), Hyogo 679-5148, Japan
[k] Dhaka Institute for Materials Science (DIMS), University of Dhaka, Dhaka 1000, Bangladesh
[l] Western Australian School of Mines: Minerals, Energy and Chemical Engineering, Curtin University, GPO Box U 1987, Perth, WA 6845, Australia

ARTICLE INFO

Keywords:
Solar-energy
Solar water heater
Thermal collector
Nanofluids
Sustainable development

ABSTRACT

The solar water-heating (SWH) system is one of the most convenient applications of solar energy, which is considered an available, economical, and environmentally friendly energy source to fulfill the energy demands of the world. In this review, existing SWH systems and design aspects of major components e.g., solar thermal collector, storage tank, heat exchanger, heat transferring fluid, absorber plate, etc. were extensively studied. Recent research to further improve SWH systems and potential practical applications are critically reviewed. Moreover, a relatively new concept in SWH systems, which is using nanofluids in solar collectors as heat transfer fluid has been studied in terms of design criteria for the development of SWH systems. Stationary flat plate collector (FPC) and single-axis tracking compound parabolic collector (CPC) exhibit thermal efficiencies of 45–60 % (operating range: 25–100 °C) and 30–50 % (operating range: 60–300 °C), respectively. The use of thermal stratification structures e.g., diffusers, baffles, membranes, fabrics, etc. is an effective tool to reduce heat losses from the storage tank as well as to harvest the highest energy from the solar collector. Coating of nanomaterials e.g., nickel, copper, etc. was found to reduce the backside heat loss in SWJ systems which eventually increases the thermal performance of the system. Nanofluids consisting of multiwall carbon nanotubes (MWCNTs) and Al_2O_3 increased the effectiveness of FPC by 28.3 and 35 %, respectively. Moreover, using CuO nanofluids, the collector efficiency of a typical evacuated tube collector (ETC) was increased by up to 12.4 %. Several potential future recommendations for improving the performance of the SWH system were stated.

1. Introduction

The whole world is now moving towards the application of renewable energy sources because of the increasing demand and price of non-renewable energy sources e.g., crude oil, coal, fuel oil, natural gas, etc. [1,2]. The forecasted global energy demand will be approximately

* Corresponding authors at: Materials Science and Research Center, Japan Atomic Energy Agency (JAEA), Hyogo 679-5148, Japan (M.R. Awual); Department of Chemical Engineering, Bangladesh University of Engineering and Technology, Dhaka 1000, Bangladesh (M.S. Islam); Department of Chemical Engineering, Jashore University of Science and Technology, Jashore 7408, Bangladesh (M Z. Hossain Khan).
E-mail addresses: shahinoorislam@che.buet.ac.bd (Md.S. Islam), zaved.khan@just.edu.bd (Md.Z. Hossain Khan), rabiul.awual@dims-bd.org, rawual76@yahoo.com, rabiul.awual@curtin.edu.au (Md.R. Awual).
[1] Equal contribution.

https://doi.org/10.1016/j.solener.2023.111998
Received 13 June 2023; Received in revised form 2 August 2023; Accepted 3 September 2023
Available online 30 September 2023

46 and 30 terawatt-hours (TWh) by 2100 and 2150, respectively [3,4]. Literature reported that the current petroleum consumption is 105 times faster than renewable energy production and thus, it can be predicted that the world's fossil fuel reserve will be diminished by 2050 [3]. Therefore, the utilization of renewable energy sources is considered one of the most promising solutions for reducing global warming and achieving sustainable energy use. Among the sources of renewable energy e.g., solar energy, hydropower, wave energy, wind energy, geothermal energy, biomass, bio-energy, etc.; solar energy has been considered the most sustainable ones due to its extensive domestic and industrial applications such as the supply of hot water, drying, distillation, refrigeration, washing, desalination, etc. [5–7]. Solar energy-based applications can conveniently be utilized in the temperature range of 60–280 °C, out of which solar water heating (SWH) systems have become popular in recent decades [8].

Solar water heating (SWH) systems are very commonly used and extensively utilized in many countries for having potential solar radiation, which can be differentiated based on use [9]. Normally, for taking baths, washing clothes and utensils, a small amount of water is required, while a large amount of water is required in hotels, restaurants, hostels, hospitals, and industries including food processing, textiles, paper, and dairy products, etc., [10,11]. Typically, SWH is a non-complicated, less expensive, and efficient method of using solar energy that may supply hot water for houses in any climate [12,13]. In the SWH system, an incident solar energy is inverted to thermal energy and sent to a transmission media like water, air, glycol, hydrocarbon, and other nanofluids which act as a working fluid [14]. The solar thermal collector, heat storage tank, absorber plate with absorbing materials, and heat exchanger with heat transferring fluid are the critical components of SWH systems [15]. Several types of solar collectors e.g., flat plate collectors (FPC), compound parabolic collector (CPC), evacuated tube collector (ETC), photovoltaic-thermal collectors (PVTC), and direct absorption solar collectors (DASC) are available in the market. For domestic water heating purposes, FPC, and ETC are generally used because of their simple design and ease of maintenance [8,16]. The FPCs with rectangular absorber plate function below 100 °C, whereas ETCs with concentric glass tubes perform at temperatures above 150 °C [17]. ETCs have become relatively inexpensive and represent greater efficiency than FPCs due to high production volumes of all-glass types [16,18,19]. During unfavorable weather (cloudy, cold, and windy days), ETCs show greater performance than traditional FTCs due to having vacuum envelopes that decrease the conduction and convection losses [16].

Recently, research has been undergone to improve the performance of major key components of SWH systems [7]. Researchers have conducted several research on the improvement of absorber plate qualities, up-gradation of storage tank stratification, numerical modeling, and advancement of design parameters, etc. [20]. Other current research has been performed widely on augmenting the solar thermal system with superior absorbing materials, use of thermal heat pumps, optimization of heat storage tank size, use of single/double type absorbers, and the addition of phase change materials into the solar collectors [21]. Several studies have carried out modeling approaches such as computational fluid dynamics (CFDs) by using simulation software [22]. The utilization of nano-fluid is considered a potential heat transfer method to increase the thermal performance of the SWH system. The heat transfer characteristics of the fluid enhance after replacing the working fluid with nanofluids [23]. Nanofluids are used as an absorber to improve the heat transfer performance of the SWH system. There are several advantages of using nanofluids e.g., higher surface area, better optical characteristics, higher thermal conductivity, good stability, higher absorption and extinction coefficients. Several types e.g., metal, semiconductor crystal, metal oxides, and carbon-based nanofluids were utilized as heat transferring fluid in solar collectors. The novel thermal characteristics of nanofluids have reported a strengthened thermal conductivity in solar thermal collector and direct solar distillation. A strong relationship between the increase of thermal conductivity and the nano grain (in nanofluids) size by several reports [24]. In recent, there are several developments of nanoparticles–based solar–powered desalination processes (SPDP), which states the enhancement of thermal performance by incorporating nano particles [25]. Moreover, it was reported that the use of carbon nanotube (CNT) based nanofluids enhanced the thermal efficiency of the solar collectors by reducing both environmental impact and cooperating cost [26]. A similar trend was observed using silver (Ag), copper(Cu), gold(Au), and carbon-based nanofluids containing lower volume fractions (0.001 vol%) of nanoparticles [27]. Some limitations of using nanofluids in the SWH systems are associated with the high cost of nanomaterials, low stability, and pressure drop in the collector. These difficulties can be overcome by incorporating phase change materials within the PV/T system [28,29].

In this review, we have summarized the effects of solar collector technology in terms of the performance of the SWH systems. An in-depth interpretation of the efficiency of the three currently wide-spread solar-collectors (i.e., FPC, ETC, and CPC) with their design, structural development, and energy hybridization was performed to obtain valuable prospects of SWH systems. In addition, this review investigated different features of heat storage tank, heat exchanger with transferring fluid, an absorber plates with absorbing materials to find out the variation in the efficiency of the solar-energy systems. The impacts of different types of nanofluids were critically evaluated based on their thermal performances. The review paper will be helpful to acquire in-depth knowledge on various types of solar collectors based on their design, performance, and applications for future research work.

2. Solar water heating (SWH) system

The SWH system is widely applied for residential, hydraulic space heating installations, solar space heating, commercial and industrial applications [30]. However, some limitations have been introduced by using SWH systems. Greenhouse gas emission (GHG) is one of the major problems in energy generation from the household sector. The total household GHG emission was found in Spain at 20.4% while in the EU and USA was 7.5% and 20% in 2014, respectively. Therefore, the choice of an appropriate household water heating system can widely reduce total energy consumption, and operating and maintenance costs, and save the environment from GHG emissions [31,32]. Currently, 84% of the energy requirement for heating and cooling applications of water comes from fossil fuel and the remaining 16% comes from renewable energy [33,34]. In-home applications, SWH often replaces fossil fuels and electricity. It is the most economical and acceptable model of solar energy catchment. The system is appropriate for low-temperature applications that are below 80 °C for its few elements, low investment, and operation costs [35]. Fig. 1**A** represents the typical thermosiphon line diagram of an SWH system [4]. It is known as natural convection when the water is heated that circulates water through the storage tank and the solar collector. In this case, if the hot water removal pattern is changed, a thermosiphon stimulated current is generated for the solar radiation. It was reported that the thermosiphon SWH system uses a fuzzy model to estimate the temperature of the outlet water [36]. Additionally, several SWH systems are reviewed and categorized based on the modifications and designs. [37]. Fig. 1**B** describes an uncomplicated representation of a classic solar plate system utilizing a storage-container FPC [38].

The position/angle of a solar collector can be changed to absorb sunlight for a longer time. The solar collector should be covered by dark paint to absorb more sunshine once it is exposed to the sun. The glass cover is built of low iron tempered glass that is placed over the absorber [39].

3. Major components of the SWH system

As previously stated, there is main four parts of a SWH system, e.g., i) solar thermal collector, ii) heat storage tank, iii) heat exchanger with

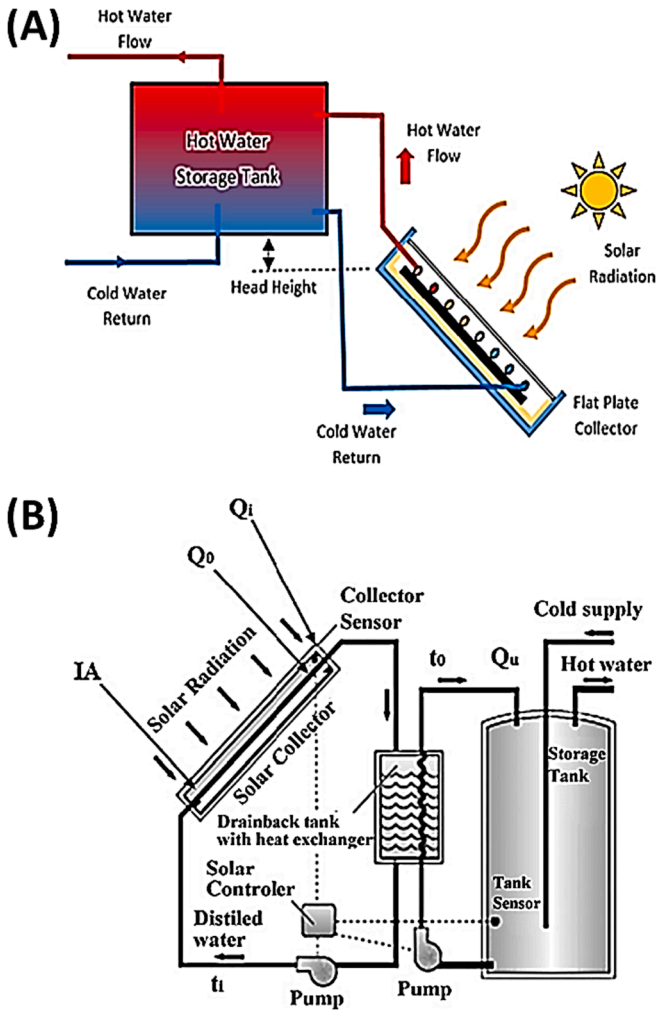

Fig. 1. (A) Typical thermosiphon SWH system. Reproduced with permission from [4] copyright, 2016 Elsevier, License number: 5596640004177, and (B) A typical solar-energy collection system. Reproduced with permission from [38] copyright, 2011 Elsevier, License number: 5596640591319.

transferring fluid, and iv) nan absorber plate with absorbing materials which has been discussed briefly based on thermal performance (Fig. 2). Additionally, various components such as a pump, piping unit, and auxiliary heating units are required for operating the SWH. The potential design and modification of major parts have been reported in respective subsections.

3.1. Solar thermal collector (STC)

The STC is considered one of the most important elements of the SWH system that absorb sunlight through the passing of a working fluid. STCs contain concentrating and non-concentrating collectors and are differentiated by the rate of sun motion and their operating temperature. These collectors are mainly relying on the intercept of the sun radiation and take up the sun irradiation in the smaller receiving area. Thus, the utilization of solar thermal energy and its application mainly depends on solar collectors [40]. The comparison of several types of STCs based on overall performance is given in Table 1.

It was reported that the design factors including volume fraction (φ), density (ρ), specific heat, thermal conductivity, specific mass, dynamic viscosity, heat removal factors (F_R) and effectiveness (F') were considerably reducing the empiricism related to the design of the solar-collector [42]. Generally, the solar-collector was inclined at a 37° angle based on a cross-sectional design that contains the matte dark color in the front face. It was reported that the increase of angle from 15° to 25°, improved the thermal performance of the collector from 27% to 30%. Furthermore, thermal efficiency was decreased from 30% to 20% by accumulating dust particles on the collector at a tilt angle of 25° [32]. The dark-painted surface was covered with glass and all other sides of the container were blocked with 5.0 cm of styrofoam sheets as shown in Fig. 3**A** [43]. A thermal diode was connected in parallel to the coated surface made of plexiglass with a strip of insulation because water can pass through it. Additionally, the thermal diode was utilized to avoid any reverse circulation of water current overnight. Santbergen et al., 2010 reported that the energy produced in just 14 s (s) by exposing sunshine which was equivalent to the energy captured by the Earth over 1000 years [44]. The use of photovoltaic thermal (PVT) system in household hot water heating is considered a promising technology due to having the analogous layout of a classic system as depicted in Fig. 3**B** [44]. Several efforts have been put to investigate the quality of absorbing solar radiation towards the efficiency of solar collectors. Direct-absorption solar collector (DASC) is another type of solar- collector where the heat transfer fluid was utilized as the absorbing media for the solar emission as an alternative to the absorber plate [45]. In DASC (Fig. 3**C**), working liquid stream between the base and the glass sheet are located at the top surface [45]. The thermal effectiveness of solar collectors (FPC, ETC, and CPC) is vital in evaluating the performance of a SWH system. A study that focuses on the design simplicity, fabrication, and effectiveness of all solar collectors is presented in Table 2.

3.1.1. Flat plate collectors (FPCs)

FPCs are the most familiar, as the cost of fabrication, maintenance, and installation is very low. Generally, there are five major parts of the FPCs namely temperature rising tube, absorber plate, insulation, fluid flow system, and the outer box. The rising tubes that are attached to the header tube are located under the absorber plate, transparent glazing cover, a black solar absorption surface, and an insulated metal or wooden box [71]. The absorber plate is made of highly selective materials so that they can absorb heat from the radiations. The fluid flow network indicates the number of rising tubes and headers which can heat the storage tank by transferring heat energy from the absorber plate. The insulated and weatherproof box is located below the dark absorber plate in order to avoid heat loss [7]. A small space is maintained between the absorber plate and the glass cover so that it can gather both diffused and direct emissions [72]. In FPC, a cover glass insulates the front part of the collector which is indicated as 'glazed' (working fluid production at 50–100 °C), while is not insulated is known as unglazed (working fluid production at 25–50 °C). The principle procedure of a FPCs is that the solar energy goes through the glass before the absorber plate and hits the flat dark-painted surface of the absorber plate at which the solar energy is captured as a form of heat by raising the inner energy [73]. In an FPC, the incident solar emission is reverted into heat and then transferred to a transport media such as water [74]. It was reported that around 80% of the sunshine was captured in FPC. Additionally, the reflected radiant heat and the heat losses in the collector surface were about 10–35% [38]. The mechanism of producing hot air or heating the water by flat-plate collectors was intensively investigated at temperatures less than 80 °C [75].

Recently, most of the researchers have focused on the progress, development, and design of FPCs. The structure of the collector is crucial factor for a SWH system [76]. The performance of FPC has been studied under steady-state and quasi-dynamic test conditions [10]. Tripanagnostopoulos et al., 2000 investigated the impact of fin attached in FTC [77]. The authors claimed that higher absorption and heat transfer coefficient was observed when the thermal energy transmits from one plate to another [77]. The impact of core components of the absorber plate in considering materials properties based on thermal effectiveness was evaluated [78]. Fig. 4**A** shows the operation of an FPC in a combination alternating heat pipe (closed-end), which provides a practically

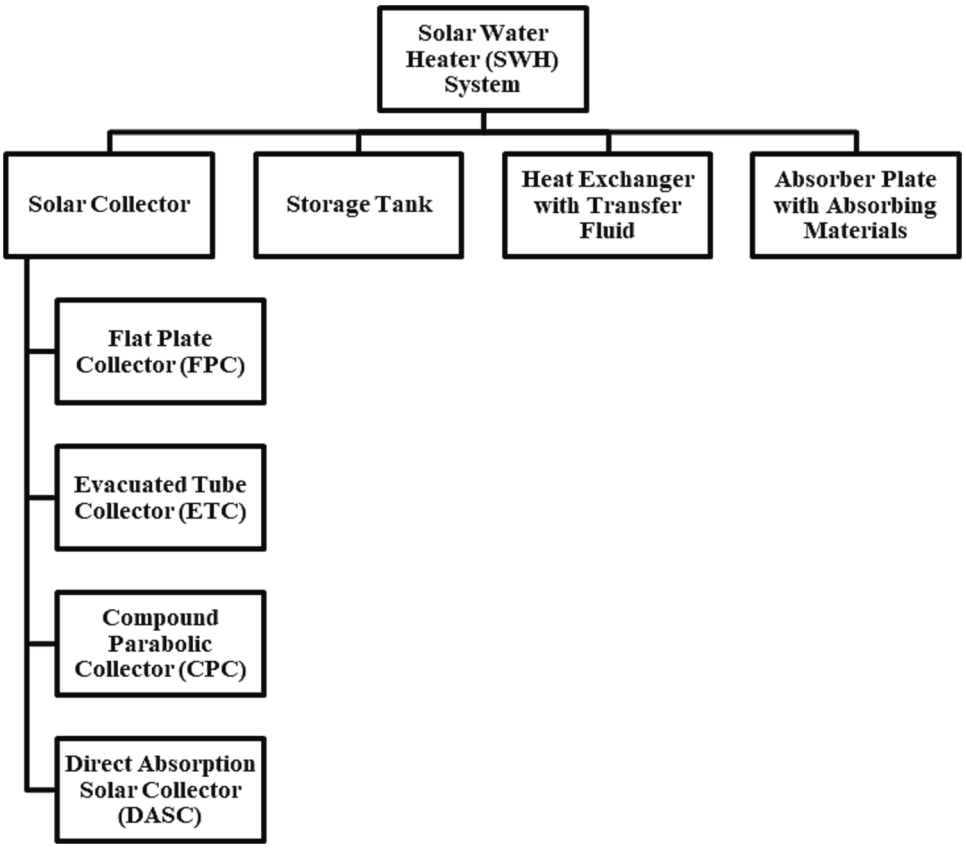

Fig. 2. Major parts of the SWH system.

effective and cost-efficient technique by using a closed-ended alternating heat pipe (CEOHP) [79]. A novel FPC containing selective coating on the micro heat pipe and attached much closer to the absorber plate was studied. The thermal performances based on three different seasons were evaluated. It can be seen that the heat gains for the three seasons were 7.42, 11.05, and 13.43 MJ/m^2, corresponding to thermal efficiencies of 50.49%, 64.25%, and 71.05% [80]. The glazing and the dark-colored absorber plate are the most important parts of a classic FPC as depicted in Fig. 4**B** [4].

3.1.2. Evacuated-tube collectors (ETCs)

ETCs are widely used STC because these can achieve higher temperatures, thermal efficiency (~84 % higher compared to FPC) and minimize heat losses in comparison to FPC [18]. Instantaneous gas heaters, solar pre-heaters, and integrated single solar tank systems are some examples of ETCs [18,19]. The production cost of evacuated tube collectors has considerably higher and gives higher efficiency than FPC because of their high initial costs. Besides, excellent thermal performance is observed in ETCs, and therefore, it represents easy transportability and installation that makes it comfortable [18,19]. Generally, it consists of copper (Cu) heat pipes for rapid heat transport, evacuated tubes to reduce heat dissipation, and an aluminum (Al) casing to supply robustness and structural integrity to the system. In this type, heat can be transported into the working fluid from the evacuated tube (metal-based). When the radiation falls on the outer tube of ETCs, it is transferred into the fluid flowing into the tube by absorbing radiation heat transfer. Generally, heat dissipation is occurred because of convection and emission [7,38].

ETCs are available in broad types, e.g., i) single-walled glass evacuated tube (SWGE) (widely used in Europe) and ii) dewar tube (DT). M. A. Sabiha et al., 2015 reported the SWGE incorporated with a direct flow type coaxial piping system and the Dewar tube with two bandles of tubes (inner tubes and outer tubes) which are made of pyrex glass [18,19]. The loss of heat energy was declined by evacuating the layer between the outer and inner tubes in DT SWH system. Some drawbacks that have originated in ETCs are the difficulty of extraction of heat from the narrow, long, and single-ended absorber tube. To address these limitations, two designs are introduced: one is the heat pipe ETC and the other is the U tube ETC [81]. Omar bait et. al. (2017) investigated the performance enhances of classical distillation unit by tubular solar-energy collector integration. It was reported that the tubular collectors can perform against a flat plat collector with lower heat loss [81]. Moreover, tubular collector-based assisted solar still was suggested for desalting saline water more conveniently than conventional solar distillation unit regarding energy, environ–economic and economic perspectives [6].

However, research is intensified on the design aspects of the ETC in the last few decades. One of the significant design criteria for the glass ETC is its shape. For instance, about 16% more energy is absorbed by using semi-cylindrical-shaped absorber tubes in ETC than FPC [82]. The thermal efficiency of filled type ETC of a U-shaped tube design was studied. In this case, diverse filling substances such as graphite and air were used. The outcomes revealed that the thermal effectiveness of the filling kind ETC was comparably higher by using graphite. The thermal conductivity of the filling layer was about 0.01 kW/m-K (Kilowatt per meter-kelvin), while if the filling substance was graphite (0.1 kW/m-K) increased thermal efficiency up to 12% as depicted in Fig. 5**A** [83]. In this ETC, each tube contains a metal absorber and a glass outer tube that was attached to a fin which absorbed the solar energy and inhibited radioactive heat losses [83]. Hazami et al., 2013 investigated the thermal performance of ETCs using water as a working fluid and compared it with the FPC. It can be seen that the proposed ETCs show a higher solar fraction (84%) than the use of FPCs (68%) [84]. The authors also reported that more energy was generated (9%) than FPCs [84]. The heat losses coefficient and the heat effectiveness factor were evaluated by

Table 1
Comparisons of different of solar heat collectors [10,40,41].

Motion	Collector type	Absorber type	Conc. ratio	Temp. (°C)	Technological maturity	Land requirement	Average Efficiency solar to thermal, %	Average Efficiency solar to electricity, %	Advantage	Disadvantage
Stationary	FPC	Flat	1	25–100	High	Low	45–60	N/A	-Low cost -Large-scale applications	-Easy to damage
	ETC	Flat	1	50–200	High	Low	30–60	N/A	-Higher efficiency -Higher operating temperatures	-Higher installment cost -overheating
Single-axis tracking	LFC	Tubular	15–45	60–250	Medium	Medium	60–80	8–10	-Higher efficiency -Low cost	-Rarely used -Used in small operational project
	Parabolic Trough Collector (PTC)	Tubular	15–45	60–300	High	High	60–80	14–16	-Low cost -Light structures	-Periodic cleaning required -Higher loss of transmittance
	CPC	Tubular	10–50	60–300	High	Low	30–50	N/A	-High efficiency –No tracking system required	-Higher reflector area -Smaller conc. ratio
Two-axis tracking	Parabolic Dish Reflector (PDR)	Point	100–2000	100–1500	Low	Low	N/A	20–30	-Easy manufacture - Higher conversion efficiency	-Storage of thermal energy not permitted -Higher cost
	Heliostat Field Collector (HFC)	Point	100–1500	150–2000	Medium	High	50–70	12–18	-Higher conversion efficiency - Capacity > 10 MW	-Relatively higher cost-Larger area (floor) required

utilizing a 1 D (one dimensional) logical solution. The investigation reported on the effect of the air layer on the heating effectiveness and noticed 10% thermal effectiveness with increasing the air layer thickness. Additionally, the temperature of the liquid was increased by 16% with containing resistivity (0.4 kW/m-K). Fig. 5**B** shows a very widely used ETC solar collector system in the current time. This is a very efficient way to heat water from the heat absorbed from the sun, however, it is costly to set up the system [85]. Teles found the highest efficiency of 42 % with a ETC made of copper and claimed the absorber temperature was maintained by the reflector at a constant level [86].

3.1.3. Compound-parabolic concentrators (CPCs)

Compound parabolic concentrators (CPC) have been extensively studied by industrial developers and academic researchers. An optical instrument interposed between the absorber and radiation source of CPC to release higher temperature. FPCs and EPCs are extensively utilized in solar thermal applications mostly to supply low to intermediate temperature ranges (20 °C to 120 °C). However, concentrators/reflectors have to be implemented to make the best use of the incident emission and thus, produce high-temperature values. Several advantages of CPCs have been formulated and a maximum working temperature of 150ºC is obtained due to the maximum concentration ratio [87].

The first concept of CPC was introduced as a non-imaging type of concentrator. The non-imaging concentrators are the parabolic (dome-like) concentrators geometrically that are capable to bounce the majority of the incident emission back to the absorber [88]. CPC consists of two parabolic sections. The geometrical concentration of CPCs with their different position is shown in Fig. 6**A** [88]. CPCs can be combined with other exiting collectors, which makes CPC an excellent secondary concentrator for SWH systems [87]. For industrial process heat application, the CPC incorporated with ETC exhibited superior performance by reducing the convection heat losses that results in the increased receiver temperature [89]. Some drawbacks have been employed in CPC such as the larger height of aperture and lower concentration ratio. To overcome these limitations, the geometrical design of CPC collectors and reflectors has to be redesigned. A modified design with two parabolic sections based in a common focus has been proposed, where the axes were inclined and angle was captured through their reflection as shown in Fig. 6**B** [88].

Kalogirou et al., 2004 reported the design of CPCs, where the lower part of the reflector is circular-shaped and the upper part is dome-shaped [90]. In recent years, other kinds of non-optical concentrators were developed. An original type of compound parabolic concentrator which composes of several rounded surfaces that can supply forward bouncing and optical light rays have been developed recently. Similarly, Kaiyan et al. (2011) investigated the diagram of this developed system that consists of dome-shaped and flat contours are known as optical concentrating parabolic collectors [91]. In this system, the bouncing beam was transferred forward from the entry opening to the exit opening as an alternative to being transmitted in the opposite direction, as the case in the traditional parabolic concentrator. This new type of CPC has increased the concentration ratio and decreased the height and angle [91]. The design of the receiver and reflector was modified so that these can be used as storage devices in the CPC. In this case, the reflector and receiver consist of three parts as a horizontal axis, a vertical axis, and a concave, and contain two concentric cylinders [92]. Recently, 3D CPC was gained more attention in the SWH system. It was reported that the impacts of 3D/2D CPC with spherical receiver containing geometrical concentration ratio (1.8) were studied, and the 3D CPC performed superiorly [88]. Dai et al., (2011) compared the 3D CPC with a single DC (dish concentrator) and two-stage solar formulated DC [93]. The impact of the air gap between the reflector outer surfaces of the absorber was

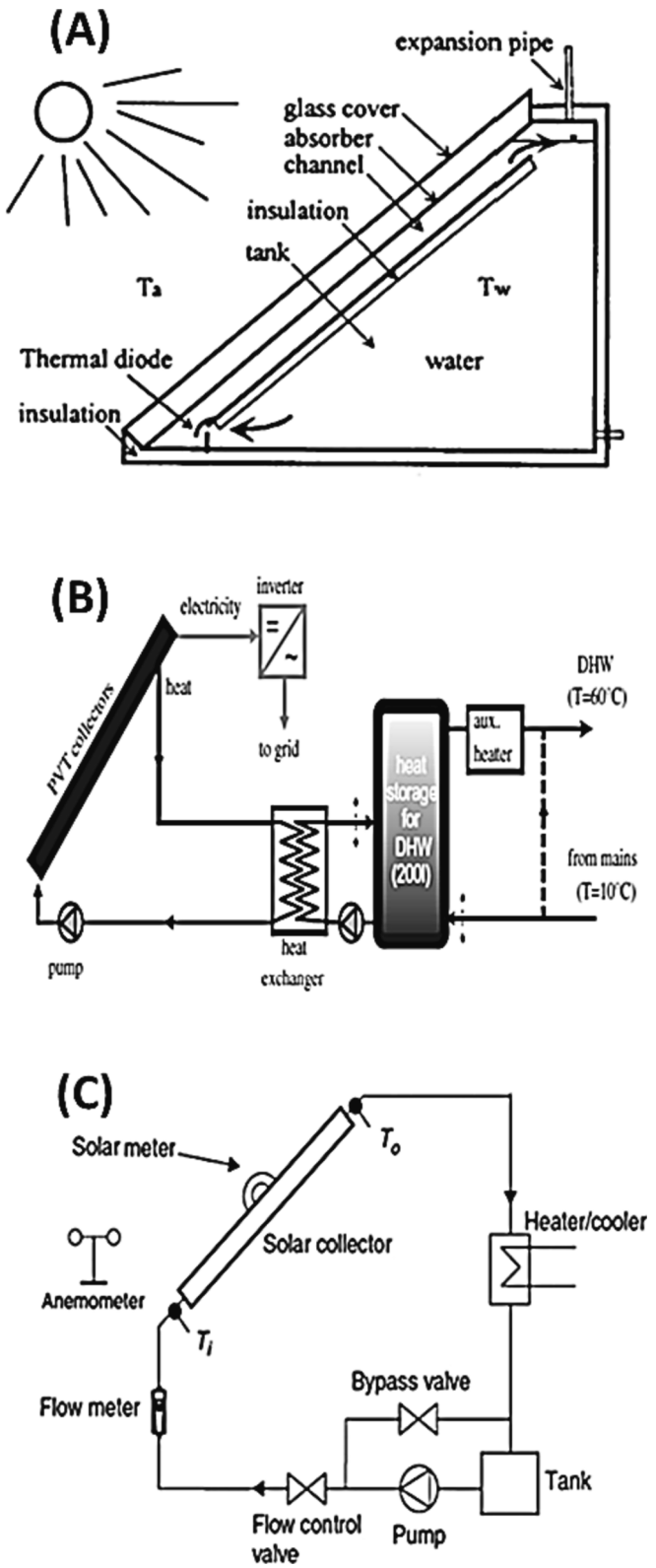

Fig. 3. (A) Schematic of the thermal diode integrated solar-collector-storage-container system. Reproduced with permission from [43] copyright, 2016 Elsevier, License number: 5596641069497, (B) PVT system for household hot water. Reproduced with permission from [44] copyright, 2010 Elsevier, License number: 5596641436987, and (C) A DASC setup. Reproduced with permission from [45] copyright, 2015 Elsevier, License number: 5596650242783.

introduced in CPC to suppress the heat loss from the sidewalls of the SWH. A comparative study was conducted with a similar model but the air gap has revealed greater performance. The highest temperature difference of water was found at 29 °C and 14 °C for with and without air gaps, respectively. The average thermal collector efficiency was increased by about 24.6% for applying air gap on the side walls of the CPC was studied [94].

3.2. Solar heat storage container and its effectiveness

Solar heat storage container is an important part of the SWH system, as it does the main function of assessing the system's effectiveness [40,95]. The temperature change of the heat storage medium (liquid or solid) is the measurement of the sensible heat storage in a SWH system. The liquid state heat storage medium (25ºC to 850ºC) materials are oil, molten salts, water, and liquid metal, whereas solid-state (200ºC to 1200ºC) materials are usually concrete, sand-rock minerals, and fire bricks [96]. Moreover, heat can be stored chemically in chemical substances through exothermal and endodermal reactions, whereas melting or gasifying phase change material (PCM) offers the possibility to store the latent heat through the reconstitution of PCM to internal phase structures [97]. However, some drawbacks have been formulated in three heat storage technologies (sensible, chemical and latent). The lower heat capacities of the materials and safety issues of the oil-based working fluid cause complexities in sensible heat storage. The PCMs with latent heat storage are required to adjust some advanced heat transfer strategies due to lower thermal conductivity. Besides, heat storage of chemicals, selection of chemical reactor, maintenance of the stability, and reversibility are required in the chemical heat storage system [40]. Generally, it is constructed using concrete, steel, plastic, fiberglass, or other suitable materials that are suitable for storing hot water. Steel is the most commonly employed material among the aforementioned materials because steel containers are easy to install [38]. Heat loss is the major problem employed in heat storage tanks because of mixing cold and hot fluid. The use of thermal stratification structures (such as diffusers, baffles, membranes, and fabrics) is an effective tool to reduce such losses as well as to harvest the highest energy from the solar collector [7].

Recently, design of the storage tank in the SWH system has been revolutionized by different advanced technologies. Diverse inlet designs of the storage container were put forward to enhance stratification. A schematic of the cross-sectional view of an improved design of the storage tank is shown in Fig. 7 [7]. The consequence of 12 diverse obstructions on the thermal stratification in a cylinder-shaped storage container by forecasting the heat allocation inside the container was studied. Additionally, the geometry of the 12 different obstacles was also evaluated. It can be seen that putting an obstruction in the container improved the thermal distribution compared to having no obstruction. The obstructions that have a space in the center (number 7, 8, and 11) also enhanced thermal distribution than those that had a space close to the container wall. In terms of hot water supply, the study concluded that obstruction 11 offered the greatest thermal distribution in the container [95]. The development of a storage tank was studied in the SWH system based on phase-changing materials (PCMs) [98]. Various types of PCMs are used in heat storage systems. It was observed that the paraffin wax-containing aluminum container gives the benefit of 13/14 °C to the water in the storage tank [7].

The effect of the depth of the storage container was carried (collector area/volume) in 120 days using 60 mm and 80 mm heaters. The lowest and utmost temperatures that were collected for the 60 mm heater were 46 and 76 °C, respectively, as the equivalent temperatures for the 80 mm heater were 41 and 70 °C, correspondingly. The average daytime utmost efficiencies of the 60 mm and 80 mm heaters were 65 and 73%, correspondingly, with a dissimilarity of 8–10% during the surveillance time [99]. Nam et al. (2014) investigated the effect of thermal loads in multi-use heat pump based SWH with control apparatus [100]. The on/off

Table 2
Different studies on the design, operation, and thermal performance of solar-collectors.

Location	Operational design	Working fluid	Outlet Temp., (°C)	Area of Collector, m^2	Mass flow rate	Title angle,	Solar irradiation, W/m2	Collector Efficiency, (%)	Main findings/ outcomes	Ref.
Flat plate collectors (FPCs)										
Salem, Tamilnadu, India	-V-cut and square-cut twisted tape. -Black coated absorber plate. -Two reflector plates are fixed at 120° inclination.	Water	40	1.0	2.6 m/s	12°	1000	8.86%	-Heat transfer increased of V through the collector was 20.1% due to fluid flow. -Thermal performance was increased 1.35 times higher as conventional one.	[46]
Gangcha, China	-Contains of three major parts: heat collector, heat storage, and cooler. -Cotton was used as insulating materials. -A water pump was connected with the water tank.	Water	50	2.0	0.03 kg/s	45°	800	4.07%	-Collectror dimensions linearly increases the thermal performance -The collector efficiency was found 4.07%, 3.56%, and 3.27% at constant solar radiation	[47]
Yekaterinburg, Russia	-Prototype FPC is made of a wooden structure. -Galvanized steel is used as an absorber plate. - Top FPCs are covered by clear glass.	Water	70	1.3	1.2 l/min	35°	1022	6.5%	-The temperature difference was reduced after 1.0 pm due to decrease of solar irradiation intensity. -The highest efficiency (66.0%) was found in 17 July 2019.	[48]
China	-FPC with V-corrugated absorber. -Aluminum, Mineral wool, and polycarbonate was used as an absorber, insulating materials, and glazing materials.	Water	69	N/A	0.1–5.3 m/s	9-53°	79.6–849.7	1.1%	-The heat gain of V-corrugated absorber plate was 64.9%. -The results indicated that long-term thermal performance of V-corrugated FPC was similar in accuracy level.	[49]
N/A	-FPC with helically corrugated tubes. -A copper absorber with black carbon-coated. -The absorber was connected with bottom and top headers	Water	N/A	0.5824	2–4 m/s	45°	800–1100	61.59%	- The highest thermal efficiency of FPC with corrugated tubes was 62 %. - The increase in friction factor was 64.5 % and Reynolds number was 5153.	[50]
Nanjing, China	-The FPC was fabricated with heat pipe, absorber plate (copper), an insulating layer (rock wool), glass cover, cross-flow heat exchanger, etc.	Water	65	N/A	1.9 m/s	30° and 45°	1000	69%	-The maximum thermal and instantaneous efficiency was 69% and 58.1% respectively. - Increase in absorber thickness increased the heat efficiency.	[51]
Lanzhou, China	-FPC with duel function as the water and air heater. -Rock wool and tempered glass was used as insulating and glass cover materials.	Water/ Air	60.4, and 59.8	N/A	0.024 and 0.13 kg/s	36° and 55°	300–1100	73.45%	- The efficiency was found about 73.45 for for water/air heating, 51.3 for air heating, 51.4 for water heating. -The lowest temperature differency was observed in water/air heating operation.	[52]
Beirut, Lebanon	-An array of minichannel was placed in the absorber plate The	Water	63.2	0.6	0.014–0.02 kg/s	45°	900	16.1%	-Thermal and instantaneous efficiency was rose by 16.1%,and 20.4%	[53]

(*continued on next page*)

Table 2 (*continued*)

Location	Operational design	Working fluid	Outlet Temp., (°C)	Area of Collector, m^2	Mass flow rate	Title angle,	Solar irradiation, W/m2	Collector Efficiency, (%)	Main findings/ outcomes	Ref.
	FPC consists of an array minichannels								compared to the old FPC. -Thermal loss was obtained due to space between glass and absorber plate.	
Padua, Italy	-A prototype FPC at roll band absorber with selective coating. -Collector was black coated. -Attached with a hydraulic loop.	Water	88	1.81	0.02 kg/s	60°	700–1000	N/A	-Roll band absorber showed superior thermal efficiency than conventional shell and tube absorber. -Furthermore, the thermal efficiency can be increased based on numerical model.	[54]
Evacuated tube collectors (ETCs)										
London	-ETC with flood design formation. -Black chrome plating was chosen for selective absorbing coating. –No contact between the pillars and absorber.	Water	85	N/A	N/A	45°	1000	56%	-The heat transfer coefficient decreased (7.43 to 3.65 W/m^2K), and the thermal efficiency increased (36% to 56%). -Heat losses were 9% of the predicted level between the absorber and glass.	[55]
Assam, India	Pump, tube, manifolds, storage tanks were used	Water	38	1.8	6–24 ml/s	45°	740–820	72%	– 72% of thermal efficiency and 6.1 % temperature difference was found -Within 5.45 min, the highest thermal performance was achieved	[56]
Melbourne, Australia	-ETC with diffuse flat reflector and consists of two parts.	Water	70	3.0	N/A		1000	27.9%	-The maximum thermal collector efficiency was observed 27.9% in Melbourne. -A comprehensive model was developed for annual energy savings, and found 95.8% for first zone.	[57]
Silchar, India	–Co-axial ETC with PCMs. - TiNox welding was used to coat the absorber plate	Water	80	6.4	78 kg/m2hr	N/A	1000	80%	-In sunny days, the thermal efficiency exceeded 80%, and fallen at noon. -The temperature profile of working fluid was non-linear.	[58]
China	-ETC with integrated bottom mirror reflectors. -The model is compatible with the operation in cold weather.	Water	60	7.6	N/A	23°	N/A	80%	-The total collector efficiency was increased from 60 to 80% using mirrors. -Around 20% of overheating can be minimized by using an obtuse angle in hot seasons.	[59]
Katra, India	-PCMs integrated heat pipe ETC. -The Al fins were fixed with pipes.	Water	67	0.752	N/A	45°	918–982	87.8%	-The daily efficiency was increased upto 87.80% using PCM, while 32–37% was found in without PCM. –20 l/h flow rate was optimum	[60]
Jiaxing, China	. -The round orifices in water tank were attached with the first connecting tube.	Water	80	4.97	1.6 kg/s	N/A	0–2000	59.9%	-The modified collector efficiency was increased upto 5% than conventional one.	[61]

(*continued on next page*)

Table 2 (*continued*)

Location	Operational design	Working fluid	Outlet Temp., (°C)	Area of Collector, m^2	Mass flow rate	Title angle,	Solar irradiation, W/m2	Collector Efficiency, (%)	Main findings/ outcomes	Ref.
									-The suitable inserted tube diameter 32 nm for a glass envelope.	
Katra, India	-PCM integrated ETC -Each evacuated tube was filled with stearic acid (SA) of 2.1 kg. -Each collector consists of 10 heat pipes.	Water	83	0.75	16 l/hr	45°	320–993	53.4%	- Incorporation of PCM exhibited 53.5 % of thermal efficiency -The proposed model was economically feasible	[62]
Dalian, China	-ETC is filled with double U-tubes. -The U-tube was attached with the delivery pipe.	Water	75	N/A	0.006 kg/s	45°	900	77%	-Double U-tube was 4% more efficient than single U-tube. -The thermal conductivity was found 100 W/mK	[63]
Coleraine, Northern Ireland	-Heat pipe with direct flow augmented solar collector. -The ETC with a CPC reflector was constructed and can be used as a concentrator augment.	Water	80	0.34	0.009 kg/s	60°	800	73.8%	-The minimum loss was observed ETC assisted concentrator as 2.47 Wm-2 K-1. -The heat pipe absorber had superior performance compared to direct flow absorber.	[64]
Compound parabolic collectors (CPCs)										
Merida, Mexico	-CPC was designed with a tracking system. -The CPC was composed of two identical curved reflecting surfaces.	Water	57	1.0	0.05 l/s	45°	1000	43%	-Collector energy and thermal efficiency was obtained 22%., and 43% respectively. -The proposed model was found to be economically feasible.	[65]
Tianjin, China	-The CPC was attached with the tube receiver. -Double glazing vacuum plates covered the shape of serpentine on the insulation layer.	Water	85	1.53	0–0.8 kg/s	30°	360–835	60%	-Thermal collector efficiency was obtained by 60%. -Most of the diffuse radiation was exploited. -High suitable in cold climate conditions.	[52]
Hefei, China	-CPC with a U-pipe. -It consists of one circulating pump, storage tank, and other components. -Storage tank was wrapped in polyurethane foam.	Water	95	2.0	N/A	36°	671–704	49%	-The thermal and energetic efficiency of collector was obtained by 49%, and 4.62% respectively, with maximum outlet temperature of 95 °C.	[66]
Merced, USA	-CPC with a non-imaging reflector. -The CPC consists of an evacuated tube receiver which was selectively coated.	Water	80	4.56	0.075 kg/s	40°	720–1000	62%	-At optimum conditions, 50% (thermal), and 62% (optical) performances were obtained respectively. -The geometric efficiency was observed at 93% compared to an ideal CPC.	[67]
Mexicali, Mexico	-CPC attached with a tracking system. - Tempered glass cover, and polystyrene based insulator was used in the CPC	Water	72	0.58	0.021 kg/s	32°	900–1000	10%	-About 10% efficiency was increased by using proposed structure and outlet temperature increased 4° than simple simple receiver.	[68]
Sendai, Japan	-The glass tube thickness was assumed to be thick.	Water	N/A	0.158	N/A	22°	800–1000	47.8%	−47.8 % of thermal efficiency was obtained. -Better performance	[69]

(*continued on next page*)

Table 2 (*continued*)

Location	Operational design	Working fluid	Outlet Temp., (°C)	Area of Collector, m^2	Mass flow rate	Title angle,	Solar irradiation, W/m2	Collector Efficiency, (%)	Main findings/ outcomes	Ref.
Mumbai, India	-CPC with the aluminum absorber.	Water	62.2	5.88	45 l/min	45°	205	39%	was found in modified CPC than conventional CPC. -About 39% thermal efficiency was obtained -Flow rate and solar intensity directly increased the efficiency	[70]

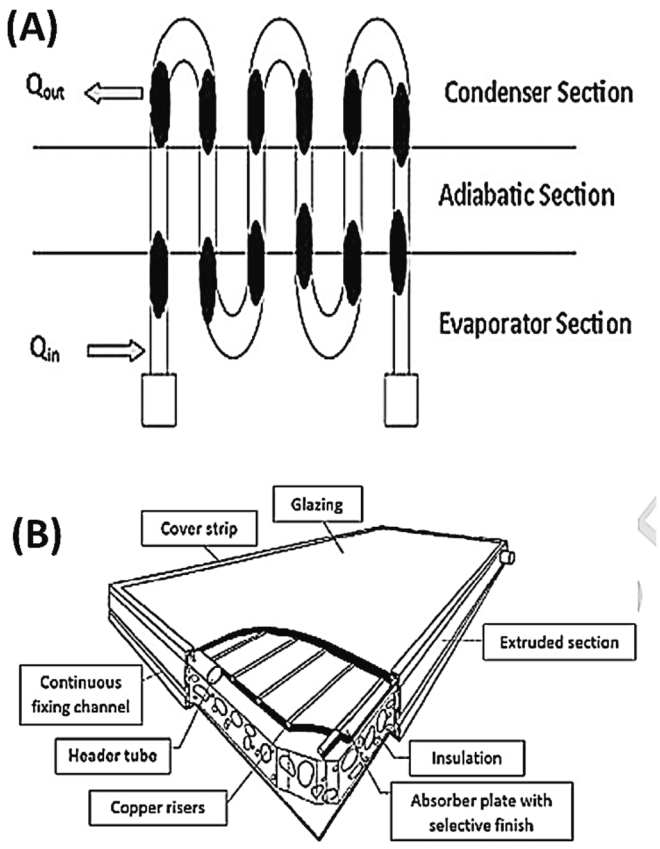

Fig. 4. (A) Closed-end oscillating heat pipe. Reproduced with permission from [79] copyright, 2013 Elsevier, License number: 5596650977331, and (B) A typical liquid flat plate collector. Reproduced with permission from [4] copyright, 2016 Elsevier, License number: 5596651217430.

control decreased power consumption about 11.2% by reducing the heat pump operation (12.2%) and variable flow rates outperformed the constant flow rate [100]. The investigation of molten salt mixtures for high-temperature thermal energy storage systems was studied. The temperature had risen to 700 °C by using low-cost storage materials of NaCl-KCl-$MgCl_2$ [101]. The detail of a study that focuses on the design, fabrication, and efficiency of the storage containers is provided in Table 3 [102–107].

3.3. Heat-exchanger and transfer fluid

The heat exchanger is the major part of the SWH system. Typically, in a heat exchanger mechanism, the captured solar thermal energy from the working liquid in the storage tank works as a heat transfer tool that is utilized to transport heat for the indirect- type of SWH system. Generally, it is fabricated from excellent high corrosion-resistant materials and thermal conductivity including copper, steel, stainless steel, aluminum, cast iron, bronze, etc. Copper is commonly utilized in the SWH system which ensures high-quality thermal conductivity and corrosion immunity. For indirect-water-heating storage containers, several configurations of heat exchangers e.g., coil-in-container, mantle thermal energy exchangers, etc. have been designed [108]. Numerous designs of the coil-in-container heat exchanger were investigated and the performance of an original distributed (Container A), and the two typical containers (Container B and C) were examined as depicted in Fig. 8 [79].

In this system, an improved inner storage design for an originally distributed storage container (A) was selected and contrasted with the widely utilized designs B and C. The thermal energy exchanger contains container B which was twisted from the bottom to the top of the container. While container C which contains the heat exchanger was twisted from the bottom to the top of the container and then U-turned downwards the bottom of the container. Finally, the distributed container was improved by 32% more when contrasted to the commercially obtainable container [79]. Tse et al. (2015) designed the conventional water heater into a ring-type heat exchanger to reduce the frictional loss for the improvement of the efficiency of the SWH system [109]. The impact of single and double-row heat exchangers with different lengths in SWH has been investigated. The thermal efficiency of double-row heat exchanger is not better than the single-row heat exchanger. Additionally, no impact of collector tilt angle based on the performance of the heat exchanger was evaluated [110].

To accumulate the thermal energy from the collector and then transport it to the storage container is performed either directly by utilizing a heat transfer liquid or with the help of a heat exchanger. In SWH, heat-transferring fluid sends the heat through the thermal energy exchanger to the water in the storage container by absorbing the energy from the collector [111]. The heat transfer fluid must have an elevated thermal conductivity, high specific heat capacity, high precise thermal energy capacity, low thermal expansion coefficient, low viscosity, anti-corrosion property, low thermal growth factor, and cost-efficient in concerning higher effectiveness of the SWH system [4]. Several examples of heat transfer fluids can be identified such as water, silicone oil, methanol, ammonia, water mixture/glycol, acetone, hydrocarbon oils, air, and refrigerants/phase-change liquids are the common heat transfer fluids. Among those, water is the most widely used fluid in the SWH systems because of its cost-efficient, low-viscous, non-toxic, non-corrosive, easily obtainable, and thermally competent liquid [112,113]. Some drawbacks have been formulated at high temperatures, water possesses difficulty in the configuration of collector plumbing and tubing, because of its corrosive nature as well as scaling and freezing issues [4]. Another heat transfer fluid air is advantageous over water because of its corrosive immunity and has no freezing/boiling issues. It is not utilized for household water-heating applications; since it has an extremely low thermal energy capacity and is very limited for applications operating at low temperatures. Alternatively, glycol is utilized with water to function

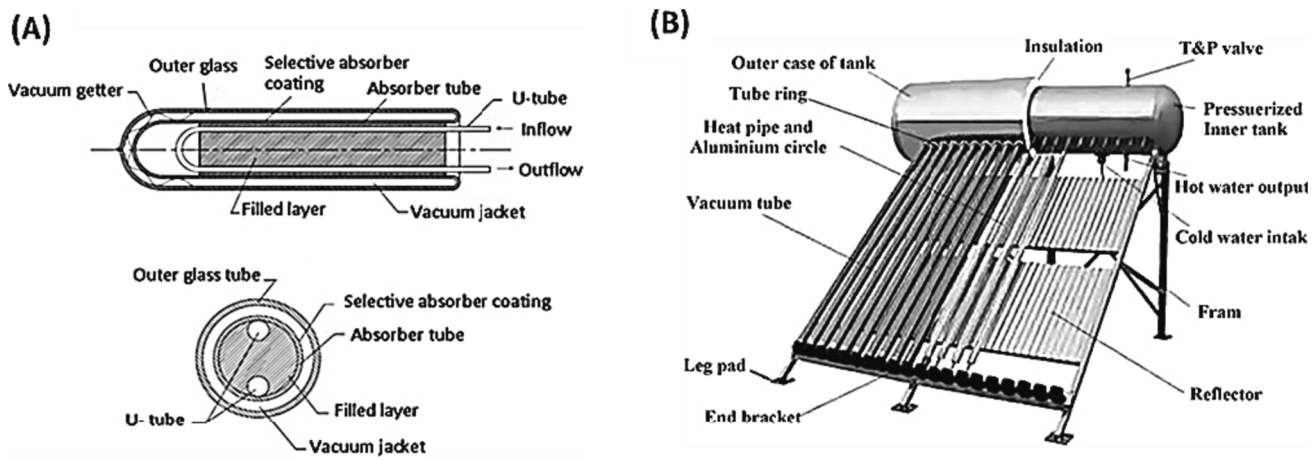

Fig. 5. (A) The filled-type evacuated tube solar-collector. Reproduced with permission from [83] copyright, 2020 Elsevier, License number: 5596651476314, and (B) Evacuated tube solar water heater collectors. Reproduced with permission from [85] copyright, 2016 Elsevier, License number: 5596750701640.

as antifreeze to overcome high freezing points relatively. In heat pumps, air conditioners, and refrigerators, refrigerants are generally utilized as thermal energy transfer liquids. Several research groups investigated the possibility of introducing a two-phase heat transfer process as an effort to enhance the operating conditions of SWF systems. The basic thermal effectiveness of two thermosiphon solar collectors with the assistance of acetone and benzene (pet ether) was investigated [4,114,115]. The effectiveness of solar-assisted heat pump was investigated both in theoretical and practical manners. The coefficients of the heat pump and the inclusive system performance, the thermal energy transport rates of the condenser and the evaporator, and the collector performance are computed for diverse container temperatures. The experimental result demonstrated that the evaporation temperature was changed between 5.2 and 20.7 °C, while the container temperature changed between 9 and 35 °C. It was observed that the evaporation temperature increased with the increase in container temperature and showed a linear change in progress. As a result, the authors suggested not allowing higher temperatures (more than 35 °C) of the container since the compressor can be damaged by operating beyond. The inclusive coefficient of the performance, theoretical and experimental values of the enhanced system with the vapor-state temperature obtained an utmost value at 5.56, 6.33, and 6.38, correspondingly. The coefficient of performance was enhanced with the increase in evaporation temperatures. The finding might be the higher heat transfer rate in the evaporator than that of using a condenser. Furthermore, the practically achieved heat transfer rates in the evaporator and condenser were 4.95 and 5.87 kW, correspondingly, and the effectiveness of the evacuated tubular solar-collector changes between 0.807 and 0.728. This is probably caused by an increase in the mass flow rates and the enthalpy variations between the evaporator's inlet and exit. Therefore, a good-agreement was shown between the experimental and theoretical results [116].

3.4. Absorber plate and absorbing materials

A coating (selective or non-selective) layer is applied to the exterior of the absorber sheet to boost the heat captured capability and decrease the radiation from the plate. The selective coatings have very high absorbance in the solar radiation range and very low emittance in the long-wave range, whereas the non-selective coatings show an inverse relation to the selective coatings. The purpose of the absorber is to enhance the solar heating capabilities and thus be considered a high-quality thermal conductor [117]. Typically, the absorber plate (collector plate) is made of Cu, Al, galvanized iron, nickel, or mild steel. Copper is considered the most suitable material for the absorber plate, because of its high thermal conductivity, however it is costly. Lizama-Tzec et al. (2019) reported that a higher thermal performance was observed by using bright/black nickel-coated absorber. Furthermore, the backside heat loss was minimized due to nickel coating that indicates maximum heat utilization [118]. However, Al is alternatively utilized, because it is comparatively less expensive (in comparison to Cu) and has a high-quality adhesion to other materials, although it has low joinability. Furthermore, high thermal performance and lower heat loss were observed with the thickness (0.005 m) of aluminum [119]. Three different collector types of absorber materials (copper, selective absorber, and galvanized sheet) were compared. The prices of galvanized absorber, copper, and selective types of heating systems in Turkey were USD 490.89, 615.69, and 740.49 per MT, respectively [120]. The absorber plate is sheltered by a dark coating using carbon powder. The coating has to be an excellent conductor and have an uneven surface to bounce the beams that are not captured. The schematic structure of a conventional solar collector with absorbing plates is shown in Fig. 9 [3].

Several factors that influence the performance of an absorber plate were studied. It was reported that the optimal size of the absorber cover and the best value of the mass current rate of the passing air should be determined for achieving the best effectiveness of the SWH system. The variety of lengths (L) and widths (b) of the dark-colored coated absorber cover was carried out in terms of several values of mass flow rate (m_f). Fig. 10**A** depicted that the outlet temperature was increased with the increase of L and b of the absorber plate. Furthermore, the effect of utilizing specific covering absorbers with their mathematical calculation was evaluated based on heater effectiveness [121]. The variations in the temperature of the absorber cover plate temperature (T_p) per hour with constant m_f (5 g/s) for diverse chosen covering materials on a hot day were performed and are shown in Fig. 10**B** [121]. Several types of absorbing materials were used in the absorber plates such as black paint, copper oxide (CuO), chromium oxide (Cr-Cr_2O_3), nickel-tin (Ni-Sn), and cobalt oxide (CoO). It can be seen that the nickel-tin (Ni-Sn) containing absorber plate exhibited a higher outlet temperature (160 °C). The chosen materials have improved values of plate absorptivity (α_p) and a lower heat transfer rate through the emission from the absorber cover to the bottom glass sheet. It was observed that the everyday average values of T_p were 120.88, 110.89, 107.18, 96.78, and 80.83 °C for Ni-Sn, CoO, Cr_2O_3, CuO, and dark paint, respectively. It was found that the thermal efficiency was increasing steadily with time. On a daily basis, the average values of thermal efficiency were observed to be 0.46%, 0.45%, 0.44%, 0.37%, and 0.33% for Ni-Sn, CoO, Cr_2O_3, CuO, and the dark painted, respectively [121]. Fig. 10**C** depicts the outcomes of the outlet temperature of the solar collector. Several coated collectors were used such as copper coated collector, aluminum coated collector, blue-coated collector, dark black coated collector, and evacuated-tube collector. The water outlet temperatures were increased throughout the test period due to capturing the quantity of energy from the sun. Consequently, the

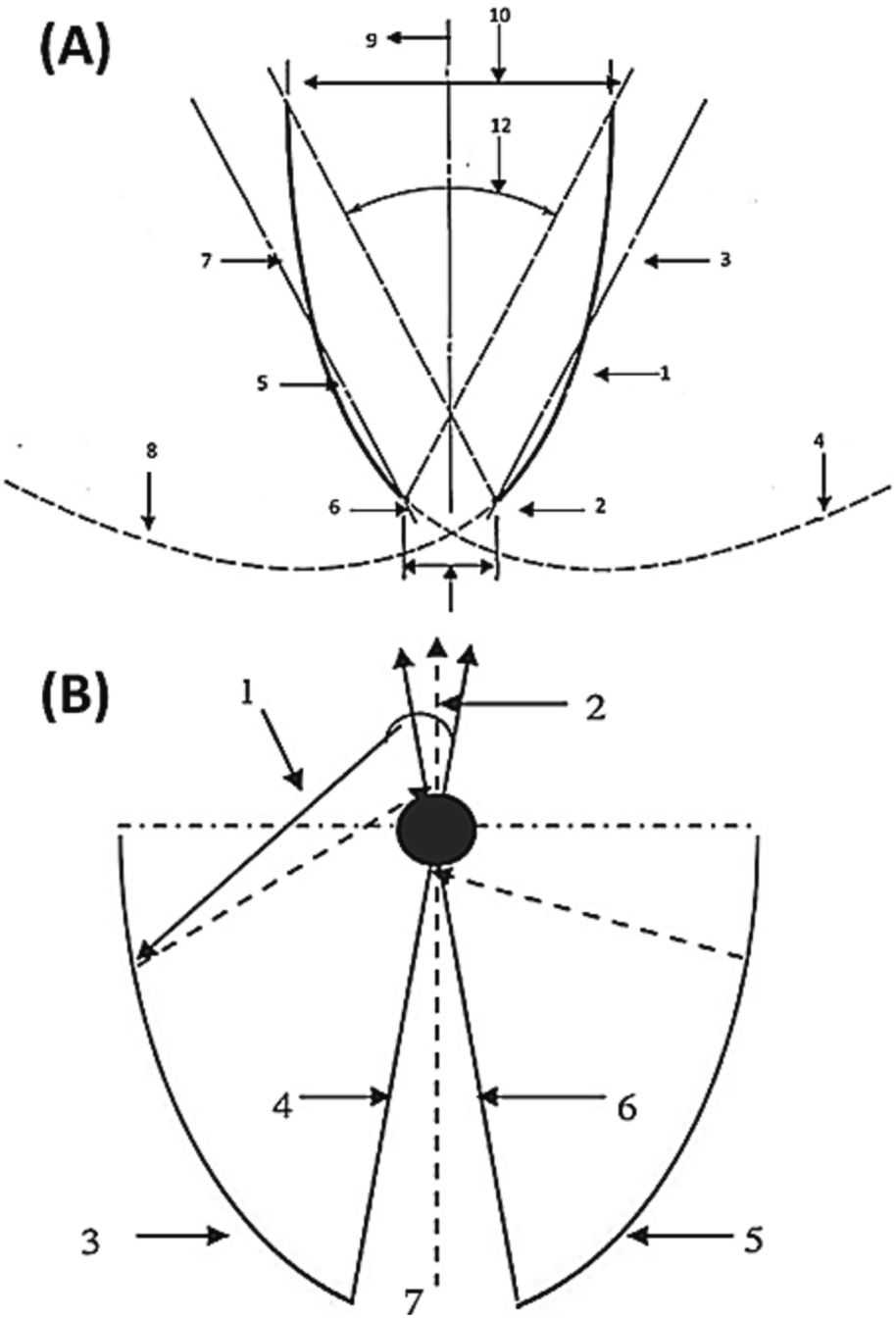

Fig. 6. (A) The geometrical components of CPC. (1) Parabola A, (2) focus of parabola A, (FA) (3) axis of parabola A, (4) truncated part of parabola A, (5) parabola B, (6) Focus of parabola B (FB), (7) axis of parabola (B), (8) truncated part of parabola B, (9) axis of CPC, (10) aperture of CPC (d_1), (11) receiver opening (d_2), and (12) acceptance angle (2α). Reproduced with permission from [88] copyright, 2013 Elsevier, License number: 5596750922127, and (B) Solar radiation incident between an acceptance angle of CPC. (1) sunray, (2) acceptance angle (2α), (3) parabola (p), (4) axis of parabola (Ap), (5) parabola (q), (6) axis of parabola (Aq), and (7) axis of symmetry of CPC. Reproduced with permission from [88] copyright, 2013 Elsevier, License number: 5596750922127.

outlet water temperature started to decrease due to lower radiation energy. It was observed that the utmost water temperature (92 °C) was found in the evacuated-tube collector, while lower in the copper collector (70 °C) at 3.00 pm. In the evacuated-tube collector, the temperature of the water at the outlet was almost 15–20% superior to that of the copper collector [122]. The instant collector efficiencies for the five collectors are shown in Fig. 10**D**. It was observed that the ETCs showed the highest thermal effectiveness than that use of black, copper, aluminum, and blue-coated absorbing materials. Moreover, the lowest effectiveness was observed when the useful heat was the lowest. At 3:00 pm, the utmost efficiencies occur and their values were 71.3%, 77.0%, 78.7%, 80.1%, and 93.5% for a copper-coated collector, aluminum coated collector, blue-coated collector, dark black coated collector, and evacuated-tube collector, respectively [122]. The special type of absorber coating called superhydrophobic was studied by Zhu et al. (2017) [123]. The sol–gel synthesized selective absorber can withstand 89.46% of the solar absorptance without corrosion. Additionally, the absorber can provide higher thermal performance even without a glass cover [123]. It was reported that the impact of concrete and sand as an absorber for household purposes. It can be seen that the attained average temperature of sand and concrete was 76°, and 72°, respectively, which indicates the concrete absorber has more outlet temperature than the sand absorber [32].

4. Application of nano-fluids in the SWH system

Recently, nanofluids have been comprehensively introduced into the SWH system. There are several advantages of using nanofluids in the SWH systems such as higher thermal properties, higher optical properties, reduce required heat transfer area, smaller size, and larger surface

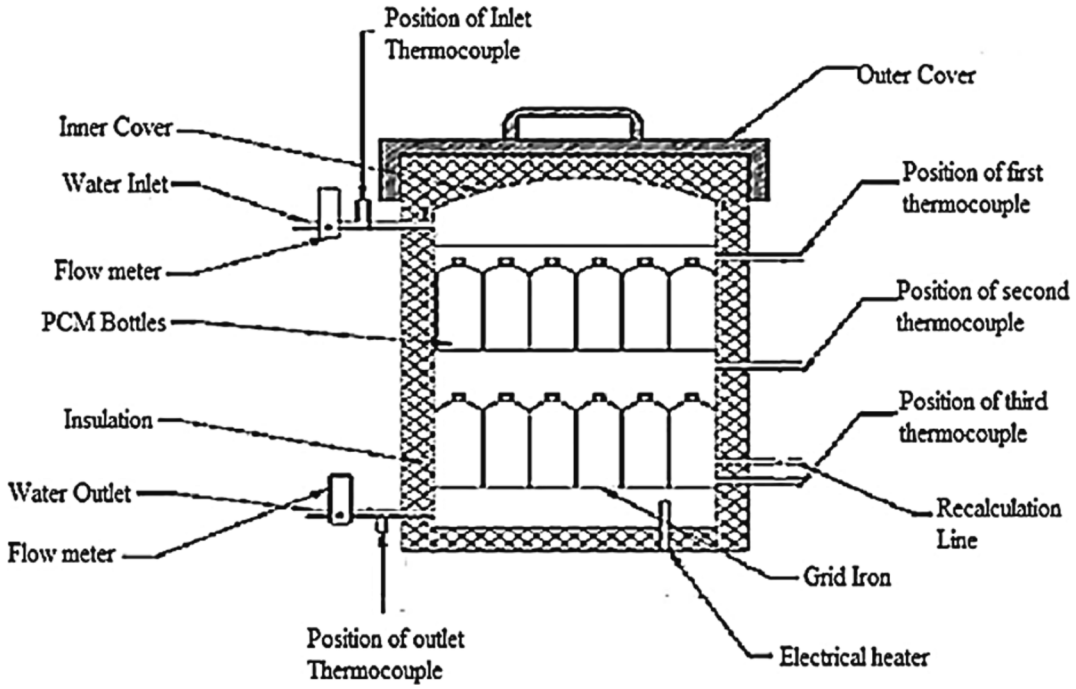

Fig. 7. Schematic illustration of a cross-sectional view of a storage tank. Reproduced with permission from [7] copyright, 2017 Elsevier, License number: 5596751044126.

Table 3
Thermal performance study of storage tank based on design, and fabrication.

Serial No	Design	Temperature Tank, T (°C)	Efficiency, η (%)	Advantages	Disadvantages	Ref.
1.	-A pipe with an opening was used as the stratified with flaps. -Flaps serve as non-return valves. -Rectangular glass tank.	51 °C	92%	-Flow rate is 5–8 l/min which is the most efficient. -Flaps reduce unwanted flow into the stratified.	- There required optimization of design for identifying the proper positioning of the partition device.	[102]
2.	-Standard mantle glass tank. - There were two draws off levels. -Two cross-linked polyethylene pipes were used as the stratified for draw-off at the top and middle of the tank.	45–50 °C	N/A	-Increased solar collector efficiency. -Better thermal performance.	- Through the lowest hole the fluid is pumped into the stratifier. -It was also act as a mixer than as a stratifying device because mixed fluid enters the tank through the top opening.	[102]
3.	-Transparent tank with 5 mm flexi glass walls. -Variable inlet design. -Unstructural meshes. -Small hemispherical baffle plate.	42 °C	70%	-Energy is higher for an ideal draw-off conditions.	-The quality of energy is minimized with poor inlet design.	[103]
4.	-Thermally stratified horizontal cylindrical tank. -Divergent conical tubes as the inlet nozzle.	42 °C	55–65%	-Cost effective in both the construction and operational phases.	-Limited to integrated collector storage tank water heating systems. -Susceptible to degradation of thermal stratification.	[104]
5.	-Horizontal divider plate with a hole in the center. -Counter flow. -Novel portioned stratified tank with lower half being preheated. −4 cm thick glass wool insulation.	35 °C	15%	-High extraction rate.	-Limited to only medium temperature conditions (60–70 °C)	[105]
6.	-Horizontal annular mantle heat storage. -Cross flow.	27–50 °C	N/A	-Large heat storage surface area. -Simple design. -Good overall heat transfer.	-Thermal stratification declined, so repositioning the inlet at a higher position is important to improve thermal satisfaction. - the connection between the collector and the tank is not effective	[106]
7.	-Heat storage with spiral groove tube bundle. -Cross flow. -Baffle plates. -Fibre glass insulation	75–80 °C	70–80%	-Superior shell-side heat transfer per unit length. -Low weight. -Low manufacturing cost. -Pressure drop comparable to the smooth tube bundle. -Considerable increase in flow rate.	- auxiliary heating necessary auxiliary heating during cloudy days.	[107]

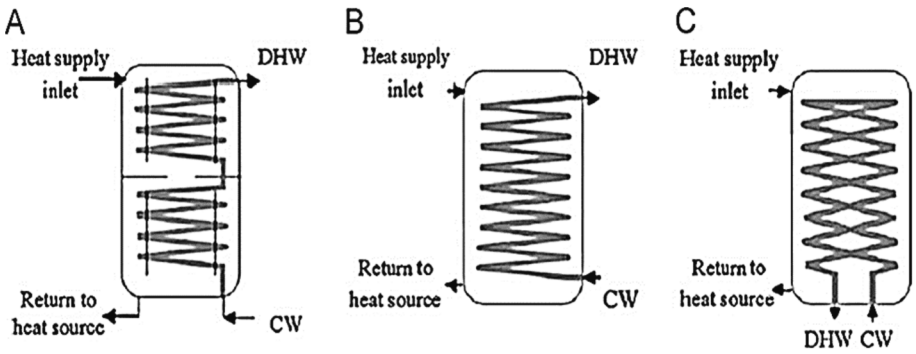

Fig. 8. Schematic designs of the coiled container heat exchanger A, B, and C. Reproduced with permission from [79] copyright, 2013 Elsevier, License number: 5596650977331.

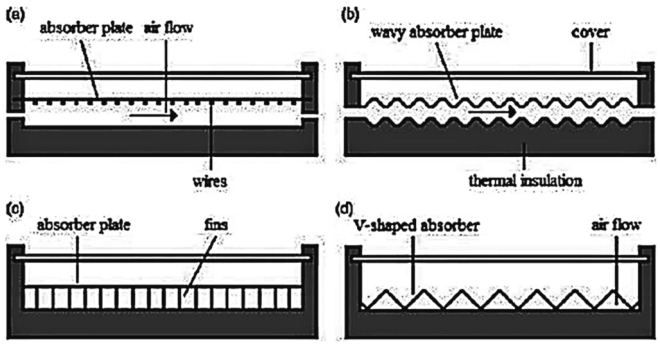

Fig. 9. Hybrid collector with absorbing plate of (A)wires, (B) wave shaped, (C) fin type (rectangular), and (D) V-shaped. Reproduced with permission from [3] copyright, 2021 Elsevier, License number: 5596751221534.

area [83]. Nanofluids application in FTCs, ETCs, CPCs, and DASCs are described briefly in this section.

4.1. Nano-fluids in SWH system

In recent times, the impact of different working fluid on the SWH system has become an interest for many engineer(s) and researchers. Extensive studies were performed to correlate the relation between the working fluid properties and system performance [124]. The incorporation of nanofluids into the absorber instead of general fluid (water) has been reported as a successful pathway to improve the characteristics of the solar collectors [18,19]. The nanofluids consist of nanomaterials and base liquid with some thermophysical and optical properties e.g., thermal diffusivity, conductivity, transmittance, convective heat transfer coefficient, and extinction coefficients [88]. It can be seen that the thermal conductivity of nanoparticles was increased due to some reasons including fluid motion, nanofluids interface, size of nanoparticles, and concentration of nanoparticles. Some key nanomaterials that have to be considered for higher effectiveness are aluminum oxide or alumina (Al_2O_3), silver (Ag), silicon dioxide or silica (SiO_2), copper oxide (CuO), titanium dioxide (TiO_2), magnesium oxide (MgO), cerium oxide (CeO_2), and the key base liquid has higher effectiveness are heat-transferring liquid in FPCs, ETCs, CPCs, and DASCs which must be given substantial concentration [6]. The first consideration is the synthesis of nanofluids. Moreover, the thermal conductivity of nanofluid can be greatly influenced by various key factors such as the size and shape of nanomaterials, which and what amount of nanoparticles are used, type of the base fluid, and annealing temperature [125]. As suspending solid nanoparticles in the base liquid will not cause a simple mix, thoroughly the stability of nanofluid must be studied [26,126]. The stability of particles can be enhanced either by alkaline/acid covalent or non-covalent interaction with the surfactant [127,128]. The stability of dispersed nanoparticles can be enhanced by adding the surfactant in the nanofluid. Another point that should be considered in using nanofluids SWH system is the cost of the nanofluids which is comparatively higher because of its preparing process [45]. The impact of thermo-physical properties of various nanofluids with respect to nanoparticles temperature and volume concentration (0.25–2.0 wt%) was studied. It was observed that nanoparticles concentration has a potential impact on the increase of thermal conductivity as shown in Fig. 11**A** [129]. It can also be seen that the viscosity of nanofluids was increased with the increased weight fraction of nanoparticles is shown in Fig. 11**B** [129]. This observation was obtained due to an increase in frictional resistance between the layer of the base fluid and the nanoparticles. The densities of nanofluids have a great impact on heat transfer performance. Similarly, another important key factor of nanofluid is the specific heat that is used to characterize the nanofluid. The density of nanofluids is dependent on nanomaterials' concentration, which increases with increasing the concentration which is shown in Fig. 11**C** [129]. Furthermore, it can be seen that the specific heat of nanofluids enhanced as the concetration of nanomaterials which is necessary for achieving higher absorption and convective heat transfer coefficient of nanofluids is shown in Fig. 11**D** [129].

Therefore, nanofluid was used to transport the utmost quantity of thermal energy from the absorber plate to the end-users by the means of enhancing the thermal properties of the working fluid which results in improving the thermal effectiveness of the solar collectors [88,130,131]. A summary of thermal performance that was reported on the use of nano-fluids in FPCs, ETCs, DASCs, and CPCs is provided in Table 4.

4.1.1. Thermal performance of FPCs using nanofluid

Numerous studies have investigated the theoretical and experimental effects of utilizing aluminum oxide (Al_2O_3) nanofluid and other carbon-based nanofluids in FPCs [159]. The influence of particle volume fraction and mass flow rate on collector's effectiveness have also been studied. The consequences showed the increase of the thermal effectiveness by utilizing the 1.5 % of particle volume fraction (Al_2O_3 nanofluid) in contrast with water as working liquid by 31.64%. It was concluded that using nanofluids enhanced thermal energy transport from solar collectors to storage containers and increased the energy density [159]. It was also believed that the effectiveness of FPCs was increased by utilizing the nano-fluids in lieu of classic heat transport liquids [145]. The impact of various nanofluids (MWCNT, CuO, TiO_2, SiO_2, alumina, and graphene) in FPCs were investigated [160]. The effect of nanofluids based on concentration and mass flow rates was performed as shown in Fig. 12 [160]. Mass flow rate from 0.01 to 0.05 kg/s enhanced the efficiency of the collector (Fig. 12**A**). However, an opposite trend was observed for energy efficiency (Fig. 12**B**). In Fig. 12**C**, nanomaterials loading from 0.25 to 2.0 vol% increase the efficiency of the collector, which required higher pumping power at higher nanomaterials loading as shown in Fig. 12**D**. The authors reported 0.025 kg/s

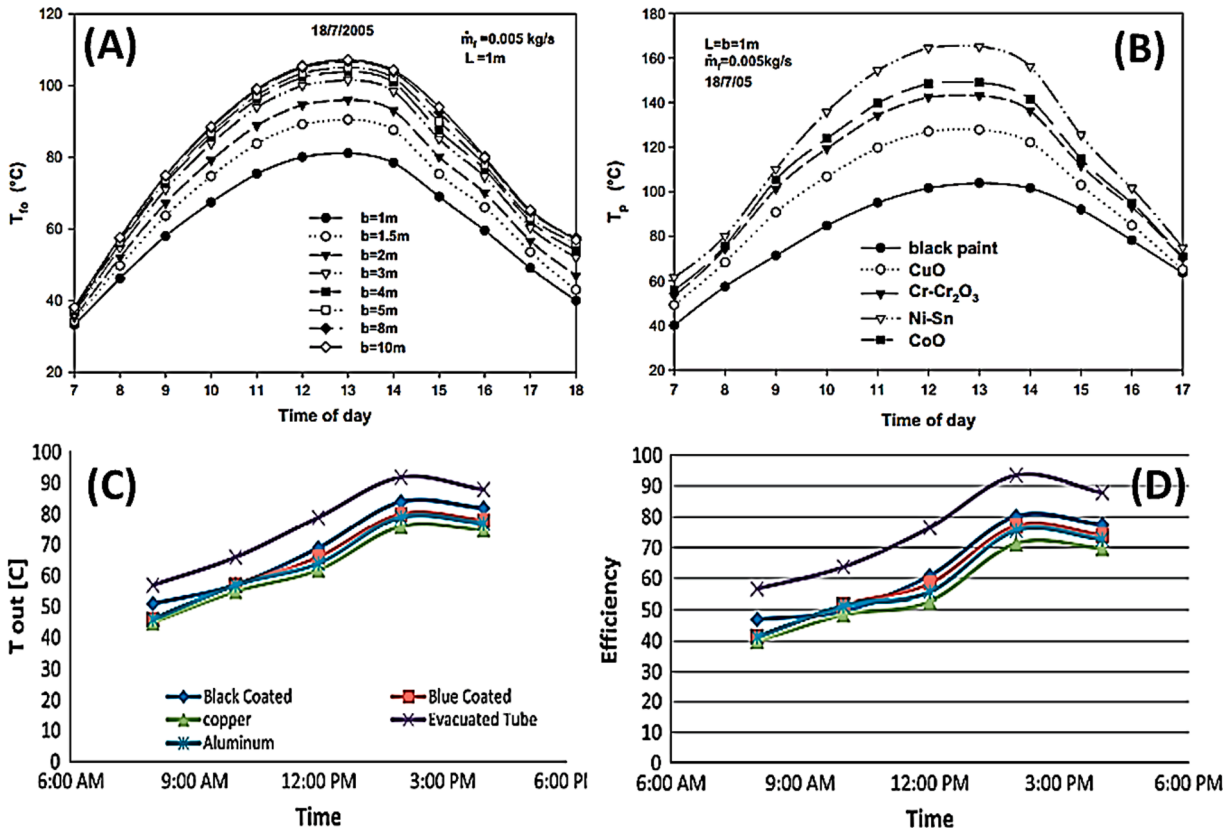

Fig. 10. (A) Effect of width b of the dark painted absorber on outlet temperature, T_{fo}, (B) Diurnal changes of temperature (T_p) for various selectively coated absorbers. Reproduced with permission from [121] copyright, 2010 Elsevier, License number: 5596751443809, (C) Outlet water temperature (April), and (D) Efficiencies of the used collectors. Reproduced with permission from [122] copyright, 2013 Elsevier, License number: 5596760084992.

mass flow rate and 0.75 vol%, of nanomaterials loading to be optimum for that operation [160].

An experimental study that focused on the influence of multiwall carbon nanotubes (MWCNTs) Al_2O_3 water nanofluid on the effectiveness of the FPCs were reported. The results showed that the effectiveness was increased up to 28.3% and 35% correspondingly using Al_2O_3 and MWCNTs nanofluids than using water as a working fluid [133,145]. In elevated flux solar-collectors, the applicability of nanofluids was investigated and it was observed that effectiveness was raised to 10% which is likely relative to a classic liquid by choosing carefully the operating conditions for 0.125% volume fraction of graphite [161]. The effectiveness of a 2 m^2 FPC was studied practically by using the effect of (MWCNTs)/ water nano-fluid as the heat transport liquid [162–169]. The operating parameters of using MWCNT nanofluids were diameter (10–30 nm), weight fractions (0.2–0.4%), and Triton X-100 was chosen as the surfactant [170]. The use of nanographene (20–30 nm) in solar collectors with 1000 W radiation source of halogen lamp provided higher efficiency and stability than the base fluid under similar conditions. The increased efficiency was observed more than 5.90% than the base fluid [171]. The authors used a Cu absorber plate with a chosen paint, an Al frame, Cu header, and riser tubes with 2.2 and 1 cm diameters, correspondingly, and 0.4 cm float glass sheet to construct the solar-collector. To mix the liquid in the forced-convection test setup, an electrical pump was used [23]. Another study reported the 0.05 wt% Cu/water nanofluid in FPCs increased 24% of collector's efficiency [172]. The thermal performances of FPCs were studied using nanoparticles including Al_2O_3, SiO_2, TiO_2, and CuO. The thermal efficiency was obtained at 21.5%, 21.6%, 22.1%, and 25.6% for Al_2O_3, SiO_2, TiO_2, and CuO nanofluids, respectively and CuO is considered an optimum choice for achieving maximum efficiency [23]. Another researcher has studied the thermal performance of FPCs by using nanofluids. The authors claimed that the efficiency was increased up to 10% and found 9 times higher incident radiation than a conventional FPCs [18,19]. Literature reported the impact of graphene oxide (GO) nanofluids in FPCs. The GO nanofluids were synthesized with variable concentration ranging from 0.005 to 0.02 vol% and considered stable after 60 days of the experiment. The highest thermal efficiency of FPC was observed (7.3%) using GO nanofluids with constant loading (0.02 vol%) and mass flow rate (0.0167 kg/s), respectively [160].

4.1.2. *Thermal performance of ETCs using nanofluid*

MWCN/water based nanofluid in ETC system with 4 % increase in collector's efficiency was reported by Tong et al., (2015) [154]. The feasibility of using CuO/water nanofluids was also investigated with an increase in 12.4% of the efficiency by Lu et al., (2011) [142]. The CuO nanoparticle concentration showed highly influential to the thermal performance and optimum mass concentration of 1.2 wt% was measured [173]. The authors claimed that the CuO nanofluids have greater potential to improve the evaporation heat transfer coefficient by around 30%. Furthermore, the surface temperature of the collector was reduced because of using CuO nanofluid [173]. A similar trend was observed to study the ETCs by using water-based CuO nanofluid. It can be seen that the thermal efficiency of ETCs has increased a maximum value (6.6%), as well as the mean value of collector efficiency, was also increased (12.4%) [173]. The TiO_2 nanofluid was used to increase the thermal performance of ETCs as compared to water.

The thermal performances of ETCs were determined theoretically by using different types of nanofluids. The nanofluids contains various concentrations in 20% propylene-glycol–water solution such as MWCNT (0.1–0.2 vol%0, SiO_2 (1–3 vol%), TiO_2 (1–3 vol%), Al_2O_3 (1–3 vol%), and CuO (1–3 vol%), respectively. The improvement of thermal efficiency for the various nanofluids with temperature differences is shown

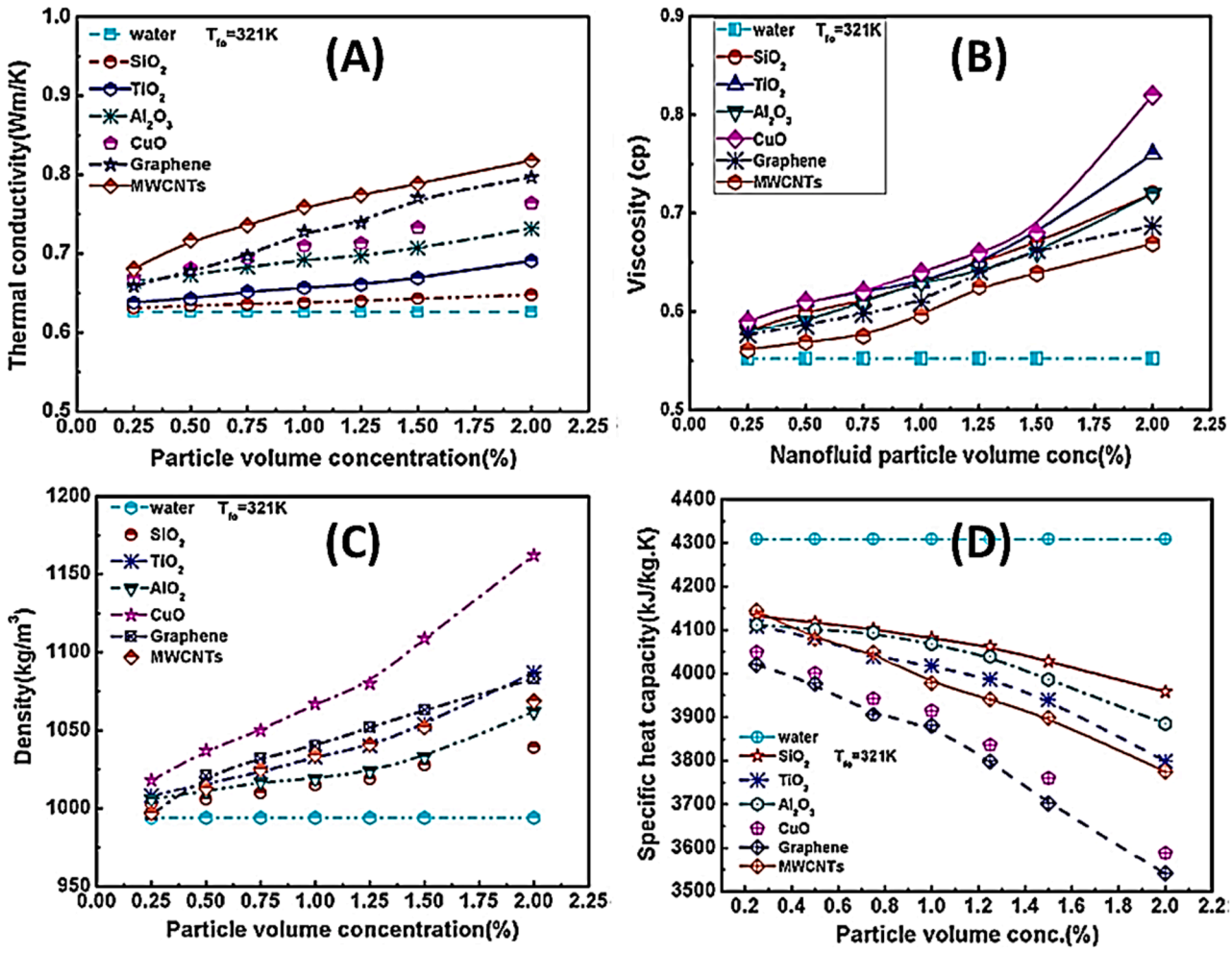

Fig. 11. Impact of thermophysical characteristics of different nanofluids with respect to nanoparticles volume concentration; (A) thermal conductivity (Wm/K) of nanofluids, (B) viscosity (cp) of nanofluids, (C) density (kg/m^3) of nanofluids, and (D) specific heat capacity (KJ/Kg.K) of nanofluids. Reproduced with permission from [129] copyright, 2019 Elsevier, License number: 5596760277415.

in Fig. 13 [174].

It can be seen that the highest thermal efficiency (62.8%) was obtained for 0.2 vol% of MWCNT nanofluid [174]. Iranmanesh et al. (2017) evaluated the thermal efficiency of the GNP/water nanofluid based ETC collector at several flow rates and volume concentrations of GNP/water nanofluid [175]. Around 90.7% collector efficiency was recorded by using GNP nanofluids with maximum concentration (0.1 wt %) [175]. To increase the thermal performance of ETCs, an SWCNT was incorporated as a nanofluid. The authors observed the maximum thermal efficiency (66%) of ETCs by using 0.2% SWCNT nanofluid than that of using conventional ones, respectively. However, the study shows an excellent heat transfer performance, but the authors did not present the impact of nanofluid stability and the pumping power of the system [160]. Hussain et al., (2015) reported the impact ZrO_2/water and Ag/water nanofluids in ETC [176]. It was observed that the thermal efficiency was improved by using both nanofluids and base fluid (water).

4.1.3. Thermal performance of CPCs using nanofluid

Operating at 150–500 °C, makes CPCs a mature technology for high temperature applications [177]. In CPC, a reflector was attached with a closed-end pulsating heat pipe (PHP) that acts as an absorber as shown in Fig. 14**A** [178]. In this case, a prototype of the collector was constructed. A novel CuO/oil based nanofluid was proposed and compared with its thermal performance of conventional CPC [179–189]. The absorption and extinction coefficient of the oil was enhanced significantly by adding CuO nanofluid. Moreover, the proposed CPC showed a higher geometrical concentrating ratio (7.36) than conventional CPC [80]. The impact of a solar adsorption refrigeration system with an increased adsorbent bed was investigated. The developed absorbent bed consists of four parallel finned tubes with their own CPC as shown in Fig. 14**B** [178].

Kasaeian et al., (2015) examined the thermal reading of CPC of four types of receivers. The experimental result revealed that the black chorme coated cupper tube absorber showed a higher absorption coefficient (0.98) [190]. This observation was found due to lower convection losses of absorber tubes [190]. The thermal performance of Cu/H_2O nanofluid-coated CPC was studied. Various operating parameters including outlet temperature, thermal efficiency, and temperature distribution were performed and compared with the conventional one. It can be seen that the addition of nanoparticles to the base liquid was improved the radiation absorption capacity of CPC [191]. The application of Al_2O_3/synthetic oil nanofluid was studied to measure the thermal performance of CPC. The authors reported the increase of particle concentration with the decrease of absorber plate size due to lower temperature gradients [192]. Khan et al., (2018) studied the thermal efficiency of CPC using Al_2O_3/oil nanofluid [193]. The experimental result showed that the collector efficiency was obtained of 23.83% by using Al_2O_3/oil-based nanofluid [193]. Similarly, the addition of Al_2O_3/synthetic oil-based nanofluid improved the relative thermal efficiency up to 11% and reduced the maximum amount of heat loss than the conventional one [194].

Table 4
Thermal performance study of different solar-collectors using nanofluids.

Type	Nanoparticles Method/ Disperse technique	Concentration	Size (nm)	Base fluid type	Area of Collector, m^2	Surfactant	Type of Collector	Mass flow rate	Title angle,	Outcomes/ findings	Ref.
Al_2O_3 ZnO Fe_2O_3	Two-step/ ultrasonication	1.0, 2.0 and 3.0 vol%	45, 60, and 30, resp.	Water	0.22	Without	FPC	1.2 l/min	30°	- The thermal conductivity was enhanced (upto 6.7 %) using Al_2O_3 nanofluid	[132]
MWCNT)	Two-step/ ultrasonication	0.2–0.4 wt%	10–30	Water	2.0	Triton X-100	FPC	0.0167–0.05 kg/s	45°	-Thermal performance was increased by using 0.2 wt% surfactant. -Also, efficiency was improved by 0.4 wt% MWCNT nanofluid than conventional one.	[133]
Al_2O_3	Two-step/ ultra-sonication	0.001–0.05 vol%	20–30	Water	1.12	Without	DASC	2 l/min	45°	- Volume concentration increase in nanofluid enhanced the collector efficiency	[134]
SiO_2	Two-step/ vertical mixing	1.0 wt%	12	Water	1.0	Without	FPC	0.35–2.8 l/ min	45°	-Volume concentration and flow showed positive impact on efficiency Temperature gradient was lower than pure water.	[135]
Al_2O_3	Two-step/high pressure homogenizer	0.05–0.1 vol%	13	Water and EG/ water 60:40	1.84	Without	FPC	0.5–1.5 kg/ min	22°	-Higher efficiency (73.7%) was observed by using smaller nanoparticles (13 nm) of Al_2O_3. -Additionally, smaller nanoparticles perform excellent in point of thermal conductivity, stability, and energy formation.	[136]
Ag	Two-step/ magnetic stirring	5–40 mg/l	20	Water	N/A	TPABr	DASC	2.5–10 m/ min	30°	-Around 58 % thermal efficiency was obtained.	[137]
CuO	Two-step/ ultra-sonication	0.4 vol%	40	Water	1.5	Without	FPC	1–3 kg/min	17°	-Overall collector performance was increased upto 16.7% by using CuO/ water nanofluid. -Maximum heat absorption coefficient was recorded using nanofluid.	[138]
TiO_2	Two-step/ ultrasonication	0.3 vol%	30–50	Water	16.0	N/A	ETC	2.0–3.5 LPM	8.2°	Temperature increased significantly in nanofluid	[139]

(*continued on next page*)

Table 4 (*continued*)

Type	Nanoparticles Method/ Disperse technique	Concentration	Size (nm)	Base fluid type	Area of Collector, m^2	Surfactant	Type of Collector	Mass flow rate	Title angle,	Outcomes/ findings	Ref.
Cu	Two-step/ magnetic stirring	0.02–0.001 vol%	25, and 50	Water	N/A	SDBS	DASC	N/A	45°	-An increase of 16.07% was obtained with 0.3 vol% TiO_2 nanofluid. -Absorption (solar) efficiency enhanced by Cu nanofluid. -Cu nanofluid sshowed excellent absorption ability.	[140]
TiO_2	Two step/ homogenous magnetic stirring	0, 0.1, 0.2 and 0.3 wt%	20	Water	1.0	Triton X-100	FPC	0.6–1.8 l/ min	55°	− 15.7% increased collector efficiency was obtained. - TiO_2 based nanofluid exhibited the highest heat transfer coefficient	[127]
MWCNT SiO_2 TiO_2 Al_2O_3 CuO	Two-step/ mechanical mixing	0.25–2.0 vol%	7 10 44 45 42	Water	0.375	Triton X-100	FPC	0.025 kg/ min	N/A	-Higher erergetic (23.47%) and exergetic (29.32%) efficiency found for MWCNT nanofluid compared to conventional one. -The surface area of collector was decreased upto 19.11% for using MWCNT nanofluid.	[141]
CuO	One-step/ ultrasonication	0.8–1.5 vol%	50	Water	N/A	Without	ETC	N/A	30°	-Heat transfer properties were influenced by using CuO nanofluid.	[142]
MWCNT	Two-step/ magnetic stirring	25–100 mg/l	10–20	Water and EG (70:30)	1.2	Without	DASC	54, 72, and 90 l/h	45°	- Volume concentration increased collector(s) efficiency	[143]
CuO	Two-step/ magnetic stirring	0.05 vol%	0.3 and 0.21	Water	2.18	SDBS	FPC	0.1 kg/s	13°	− 6.3% of increase in thermal characteristics was achieved using CuO nanofluid at volume concentration (0.05%).	[144]
MWCNT	Two-step/ ultrasonication	0.2 to 0.4 vol%	10–30	Water	1.51	Triton X-100	FPC	0.0167–0.05 kg/s	45°	−0.2 wt% MWCNT reduced the efficiency in absence of surfactant.	[145]
SWCNT	Two-step/high pressure ultrasonication	0.05–0.2 vol%	1–2	Water	N/A	SDS	ETC	0.008–0.025 kg/s	N/A	-Lower flow rate enduced greater temperature difference	[18,19]

(*continued on next page*)

Table 4 (*continued*)

Type	Nanoparticles Method/ Disperse technique	Concentration	Size (nm)	Base fluid type	Area of Collector, m^2	Surfactant	Type of Collector	Mass flow rate	Title angle,	Outcomes/ findings	Ref.
SiC	Two-step/ ultrasonication	0.01–0.06 wt%	30	Ionic liquid	N/A	Without	DASC	N/A	45°	-The performance was increased by using SiC nanofluid. -SiC nanofluid was effective (medium high temperature system).	[12]
SWCNT	Two-step/high pressure homogenizer	0.1 and 0.3 vol%	1–2	Water	1.84	SDS	FPC	0.5–1.5 kg/ min	22°	-The thermal efficiency was increased about 95.12% using nanofluid than base fluid water (42.07%). - Highest thermal conductivity (91.0%) was obtained using SWCNT for 0.3 vol% at 298 K.	[146]
MgO	Two-step/high pressure homogenizer	0.25–1.5 vol%	40	Water	0.375	Cetyl Trimethyl Ammonium Bromide	FPC	0.5–2.5 lmp	N/A	- At 0.75% volume concentration, 9.34 % collector (s) efficiency was increased.	[147]
SiO_2	Two-step/ ultrasonication	0.5, 0.75, and 1.0 vol%	40	EG/ water 1:1	1.59	Without	FPC	0.018, 0.032, and 0.045 kg/min	45°	-Increment of volume concentration of nanofluid enhanced the efficiency. - Instability problems were addressed.	[114]
CNT	Two-step/ ultrasonication	0.015 vol%	10–12	Water	1.84	N/A	ETC	0.00125 kg/s	50°	-The CNT nanofluid showed better performance at 0.015 vol% concentration. -Energy efficiency was increased at 50° tilt angle.	[6]
TiO_2	Two-step/high pressure homogenizer	0.1 and 0.3 vol%	20 and 40	Water	1.84	PEG 400	FPC	0.5–1.5 kg/ min	22°	-Collector and energy efficiency was increased using TiO_2 nanofluid. −76.6% energy efficiency was obtained for TiO_2 (0.1 vol%) nanofluid. − 6% increment in thermal conductivity.	[146]
Al_2O_3	Two-step/ ultrasonication	0.090696–0.1423 vol%	15	water	1.51	SDBS	FPC	0.2 kg/s	N/A	-Exergy efficiency was increased about 0.72% using nanoparticles based nanofluids.	[148]
MWCNT	Two step/ sonication	0.2–0.6 vol%	20–30	EG	N/A	GA	N/A	0.08 kg/s	45°	-Thermal conductivity was increased upto 30.59% using	[149]

(*continued on next page*)

Table 4 (*continued*)

Type	Nanoparticles Method/ Disperse technique	Concentration	Size (nm)	Base fluid type	Area of Collector, m^2	Surfactant	Type of Collector	Mass flow rate	Title angle,	Outcomes/ findings	Ref.
										MWCNT at 0.6 vol%.	
SiO_2	N/A	1.0 vol%	12 and 16	water	10.5	N/A	FPC	0.3 kg/s	30°	- Lower heat capacity of nanofluid caused higher outlet temperature	[150]
Al_2O_3	Two-step/ ultrasonication	0.03, and 0.06 vlo %	40	Water	18.0	Triton X-100	ETC	20–60 l/h	45°	-Thermal efficiency was increased about 58.65% at 0.06 vol% of nanofluid concentration. -Collector efficiency based on temperature was improved with the increase of volume concentration.	[151]
CuO Al_2O_3 SiO_2 TiO_2	N/A	3.0 vol%	N/A	water	2.0	N/A	FPC	1–3.8 l/min	45°	-The FPC area was decreased by more than 20 % for all nanofluids. - With CuO nanofluid, highest density and lowest specific heat was found.	[152]
CuO	Two-step/ultra sonication	0.03–0.06 vol%	N/A	Water	18.0	SDBS	ETC	20–60 l/h	45°	-The average output temperature was achieved upto 14% with CuO nanofluid.	[153]
Al_2O_3	N/A	0.01, 0.05, 0.1 and 0.5 vol%	15, 30, 60, and 90	water	2.0	N/A	FPC	0.007 kg/s	45°	-The thermal performance was increased by 37.44% using Al_2O_3 nanofluid at volume concentration of 0.5 vol%. -The outlet temperature was found 55 °C for nanofluid at fixed volume concentration.	[154]
GnP	Two step/ ultrasonication	0.0005, 0.001 and 0.005 vol%	2	water	3.6	without	DASC	0.015 kg/s	35°	− 83.24% of efficiency improvement using GnP than base fluid. - The maximum zero-loss efficiency was observed.	[155]
Cu	One step/ ultrasonication	2.0 vol%	5	water	1.8	without	FPC	N/A	N/A	- Heat transfer rate was increased using Cu nanofluids than base fluid. -Higher collector efficiency was observed by using Cu nanofluids.	[156]

(*continued on next page*)

Table 4 (*continued*)

Type	Nanoparticles Method/ Disperse technique	Concentration	Size (nm)	Base fluid type	Area of Collector, m^2	Surfactant	Type of Collector	Mass flow rate	Title angle,	Outcomes/ findings	Ref.
Ag	Two-step/ magnetic mixing	5–40 mg/l	20	Water	0.6	TPABr	DASC	5–10 ml/min	45°	- Thermal efficiency increased with the incident flux.	[157]
Cu	Two-step/ magnetic stirring	0.01–0.2 wt%	25–50	water	2.0	SDBS	FPC	140 l/h	45°	-Maximum temperature was recorded by using 0.1% Cu nanoparticle and heat energy increased upto 24.52%. -Good absorption ability was observed at Cu nanofluid.	[158]

*Aluminum oxide (Al_2O_3), Zinc oxide (ZnO), Iron oxide (Fe_2O_3), Multiwallcarbon nanotube (MWCNT), Titanium di-oxide (TiO_2), Graphene nanoplatelates (GnP), Copper oxide (CuO), Singlewall carbon nanotube (SWCNT), Silicon di-oxide (SiO_2), Silver (Ag), Copper (Cu), Carbon nanotube (CNT), Magnesium oxide (MgO), Silicon carbaite (SiC), Sodium Dodecyl Benzene Sulfonate (SDBS), Gum Arabic (GA), Polyethylene Glycol 400 (PEG 400).

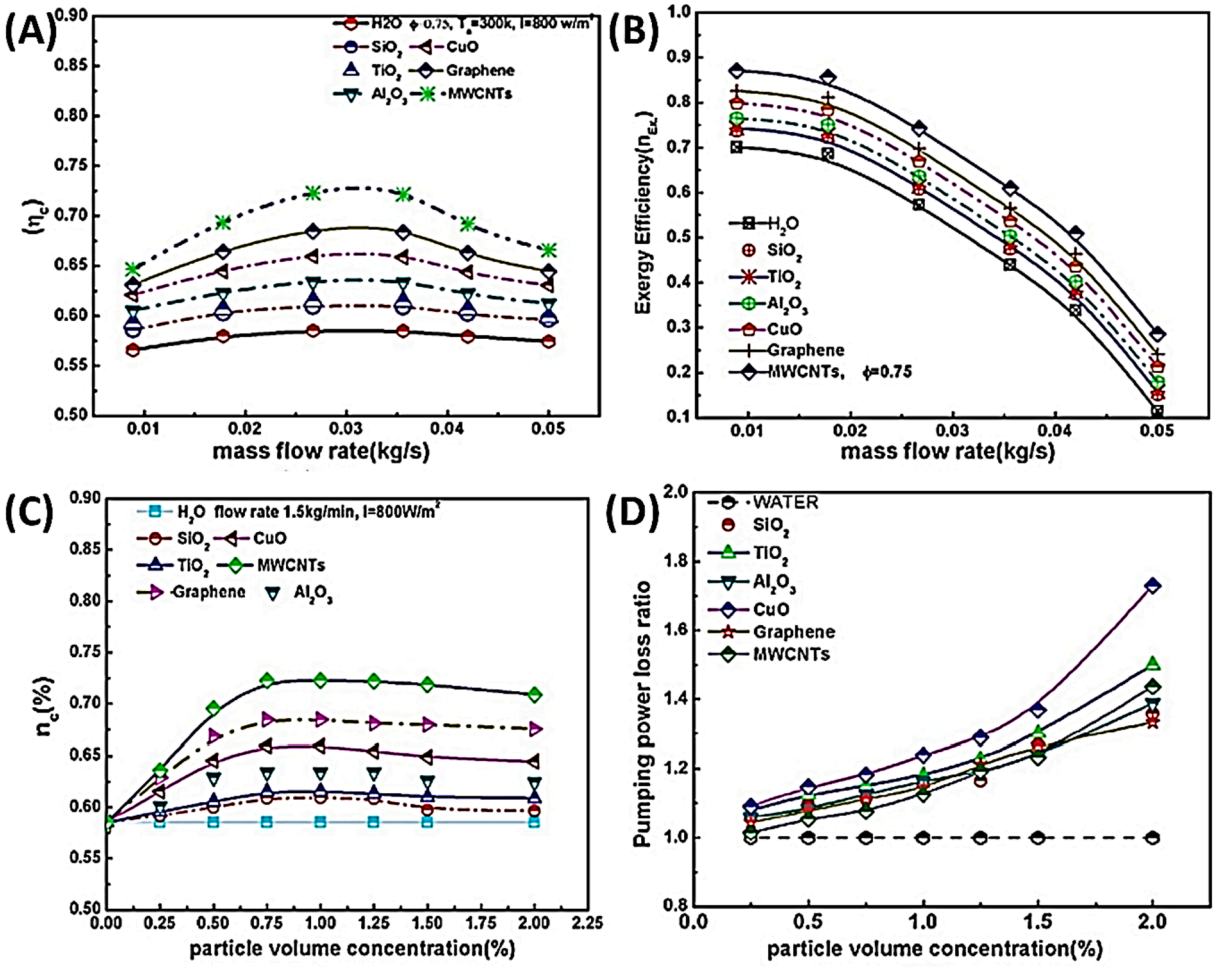

Fig. 12. Impact of mass flow and nanomaterials concentration, (A) Collector efficiency in respect of mass flow rate, (B) Energy efficiency in respect of mass flow rate, (C) Collector efficiency in respect of nanomaterial concentration, and (D) Pumping power loss ratio in respect of nanomaterial concentration. Reproduced with permission from [160] copyright, 2019 Elsevier, License number: 5596760581732.

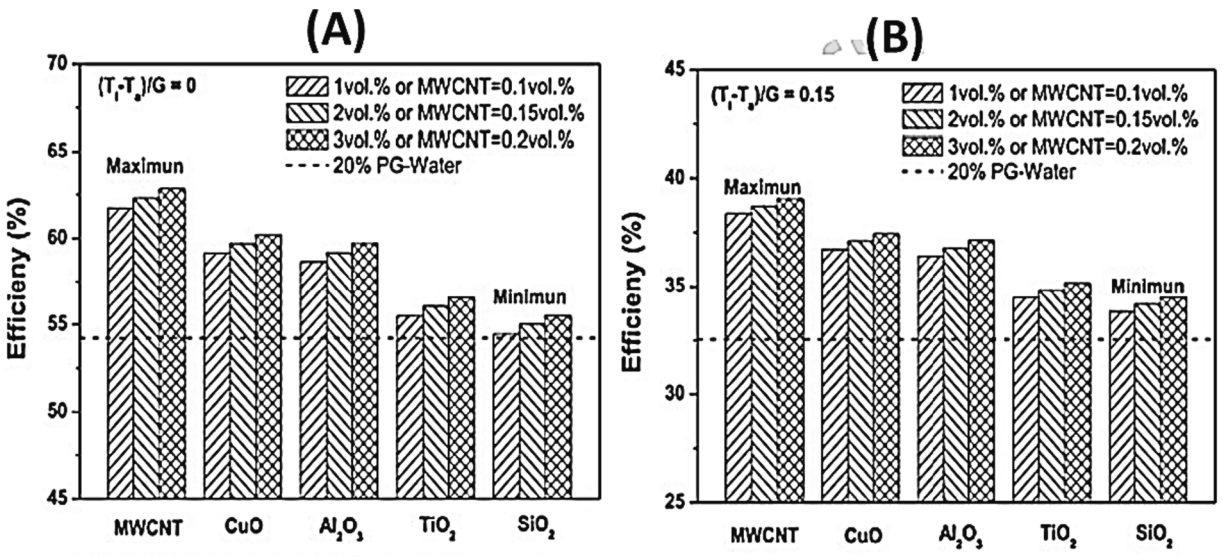

Fig. 13. Thermal collector efficiency of ETCs with various nanofluids (A) Variation in solar collector efficiency at $(T_i\text{-}T_a)/G = 0$, and (B) at $(T_i\text{-}T_a)/G = 0.15$. Reproduced with permission from [174] copyright, 2016 Elsevier, License number: 5596760777643.

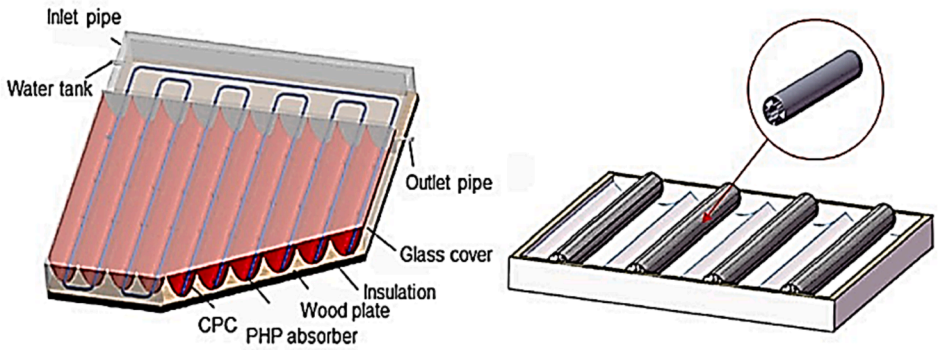

Fig. 14. (A) CPC collector, and (B) Adsorbent with CPC reflector. Reproduced with permission from [178] copyright, 2020 Elsevier, License number: 5596760939898.

4.1.4. Thermal performance of DASCs using nanofluid

Recently, several researchers have focused on the nanofluid incorporation DASCs. The nanofluid-based DASC (Fig. 15**A**) where working fluid was contained the enclosed space introduced by the transmitted solar radiation. The nanoparticles were dispersed in nanofluids by exposing solar radiation. A small portion of solar radiation was reduced through scattering the glass cover while the major portion was absorbed by nanoparticles, and converted into useful heat [160].

The utilization of nanofluids was formed by various nanoparticles such as graphite, silver, and carbon nanotube. It was reported that the collector efficiency increased up to 5% by using nanofluids as working fluids. It can be seen that the use of nanofluids improved the absorbance and decreased the reflectance of the surface as shown in Fig. 15**B** [23]. Hordy et al., (2015) investigated the use MWCNs as a working fluid in DASC [195]. The authors found excellent stability and absorbed almost 100% of the incident solar radiation with a very small amount of fluid volume [195]. Luo et al. (2014) investigated the performance of a DASC using different nanofluids such as Al_2O_3, SiO_2, Ag, Cu, graphite, and CNTs [196]. The experimental result revealed that the nanofluid-containing collector shows greater performance than the conventional one. It can be seen that the thermal efficiency of graphite nanofluid was about 122.7% for 0.01 vol% due to higher solar radiation absorption capacity [196]. Delfani et al., (2016) reported the numerical and experimental study of DASC using MWCNT nanofluid at different flow rates from 0.0150 to 0.025 kg/s [143]. The MWCNT was prepared by mixing different ratios (Water:EG = 70:30) of water and ethylene glycol. The nanofluid improved the collector efficiency by more than 10–29% than the base fluid (water) [143]. Shende et al., (2017) investigated the improvement of the thermal efficiency of DASC using reduced graphene oxide (RGO) as the absorbing medium [197]. The prepared nanofluid showed better absorption and extinction coefficient even at lower concentrations (0.005 vol%) of nanofluid [197]. The thermal properties of gold/water and MWCNT/water nanofluids at different concentrations were studied by Beicker et al. (2018) [198]. The experimental result exhibited better using nanofluids even at low concentrations than that of conventional ones. The optimum concentration was calculated and found 0.001% and 0.002% for MWCNT and gold nanofluids, respectively. It was observed that MWCNT nanofluid revealed excellent photothermal conversion ability in comparison to gold-based nanofluid [199]. Recently, RGO/water-EG nanofluid-based DASC was studied by Xu et al. (2019) and found to be 70 % efficient at 1000 W/m^2 solar intensity [200]. The author suggested that the RGO/water-EG nanofluid can replace the base fluid in DASC [201].

5. Future perspective on SWH research

Recent developments in SWH systems concentrates on an effective design utilize solar energy more sustainably and efficiently for water-heating application; to address current challenges, and focuses on the future research potentials. The most important points extracted from

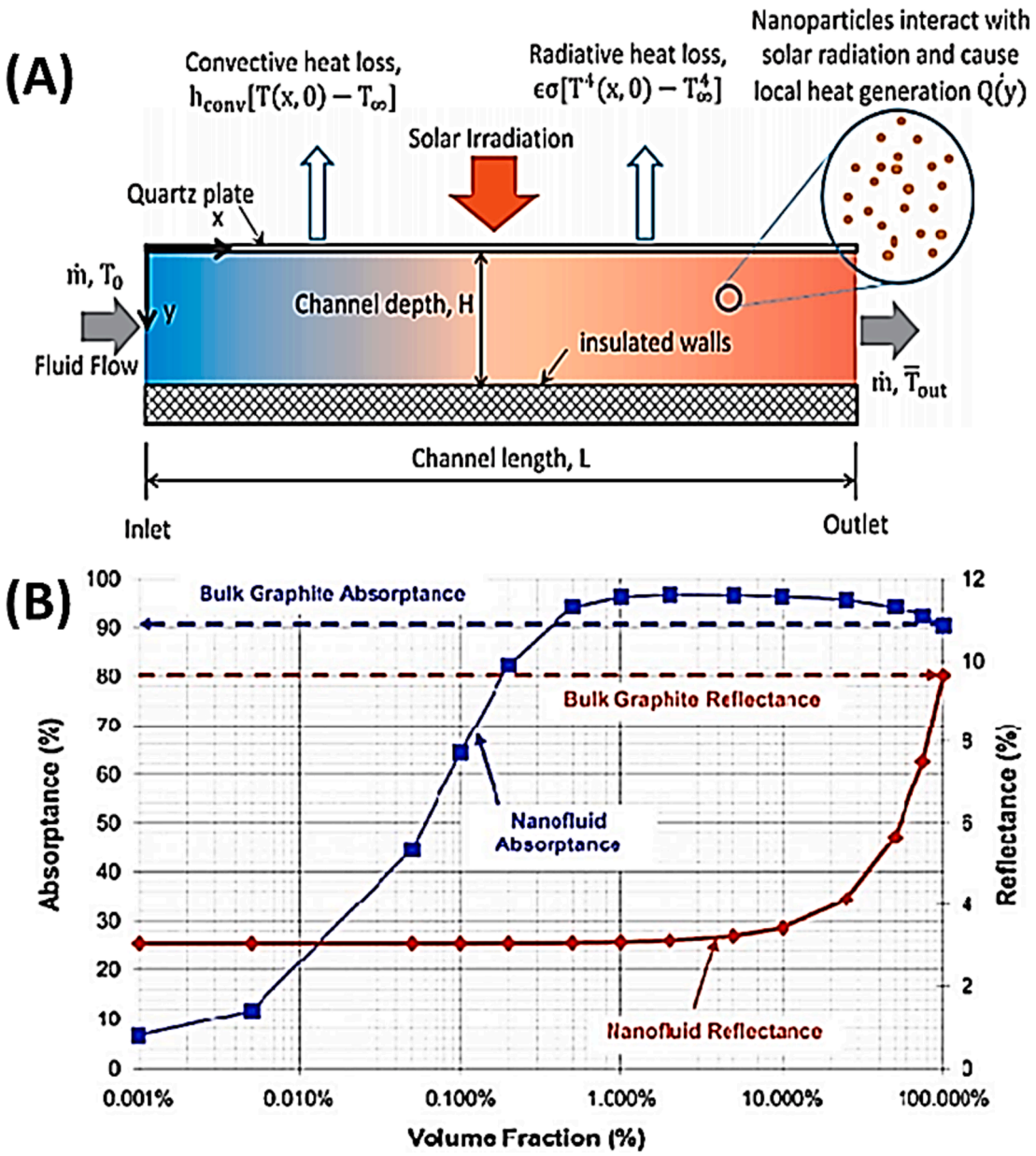

Fig. 15. (A) Schematic of the nanofluid-based DASC. Reproduced with permission from [160] copyright, 2019 Elsevier, License number: 5596761159335, and (B) Comparison and benefits of volumetric absorption of graphite and conventional nanofluid with area-based absorption. Reproduced with permission from [23] copyright, 2018 Elsevier, License number: 5596761281264.

this review can be applied for future research of SWH:

- A hybrid system can be developed in industrial applications for improving the overall efficiency by combining ETCs with CPCs that may concentrate the sunlight into a small area.
- The feasibility of using several nanofluids including phase change materials should be investigated in the SWH system.
- Thermal conductivity and solar irradiation absorptivity of the working nanofluids are two crucial parameters for the efficient operation of SWH systems.
- The critical factors, e.g., cost, size, shape, surfactant, viscosity, agglomeration, sedimentation, volume fraction, and stability of nanofluids should be considered for the large-scale applications of SWHs.
- Advanced theoretical, and experimental research are required to optimize the heat transfer mechanism in nanofluids to maximize the thermal efficiency of the SWH system.

However, despite being available in the market since 1970, SWH systems have sustained a limited growth compared to its renewable counterparts more specifically photovoltaic (PV) systems. An interesting study based on Arizona, USA remarked that educational and economic status are highly linked with the penetration of SWH systems and other renewable heating systems into the residential sectors [202]. Moreover, the residential consumers are more likely to adopt the solar PV than SWHs. Scattered information, no/low structured cost comparison, and lower level of social and government awareness programs have created a vulnerable situation regarding the adoption of SWHs in residential sectors. Thus, only concentrating onto performance enhancement of SWH systems may not satisfy the ultimate goal, therefore comprehensive studies including cost, technology, usability, and lifetime comparison of SWH systems with conventional heaters and other renewable counterparts have to be executed in different countries to get the in-depth knowledge onto the overall market status of SWH systems.

6. Conclusions

The state-of-the-art of the SWH system with design aspects of major components and potential applications of nanofluids in SWH have been critically reviewed in this article. The SWH system is the most developed and commercialized technology to transfer solar energy into thermal energy. Solar collector is the key component of a SWH system, which dominates the overall efficiency of the systems. Several types of collectors e.g., FPC, ETC, CPC etc. have been introduced in SWH systems. Thermal efficiency of ETCs can be up to 84% higher than that of FPCs, whereas CPCsn exhibit higher operating temperature range (60–300 °C) compared to FPCs (25–100 °C) and ETCs (50–200 °C). Moreover, temperature distribution characteristics of the heat storage tanks and heat exchangers greatly influent the total energy consumption in a SWH system. The incorporation of PCMs into storage tanks or solar collectors enhances thermal performance significantly. Recently, significant research(s) has been focused on the application of working fluid in SWH systems. The utilization of nanofluids e.g., Al_2O_3, Ag, SiO_2, CuO, TiO_2, MgO, CeO_2, MWCNTs, GO and base liquids exhibits enhanced thermal characteristics of solar collectors compared to the conventional working fluids, e.g., water and air. Efficiency of FPC can be increased up to 35 % by introducing MWCNTs as nanofluid. In ETCs, collector efficiency increases up to 12.4% using CuO/water nanofluid as a working fluid. The experimental result showed that the collector efficiency was obtained of 23.83% by using Al_2O_3/oil-based nanofluid [175]. Moreover, addition of Al_2O_3/synthetic oil-based nanofluid improves relative thermal efficiency by 11% and reduces the maximum amount of heat loss than the conventional nanofluid. However, there are several challenges associated with the improvements of SWH systems, which are systematically outlined in this review. To make SWH systems more sustainable, further research on the system performance and design aspects are required to raise its reliability, thermal, and cost-effectiveness.

Declaration of Competing Interest

The authors declare that they have no known competing financial interests or personal relationships that could have appeared to influence the work reported in this paper.

Acknowledgments

The authors acknowledge the support from Jashore University of Science and Technology, Jashore and Bangladesh University of Engineering and Technology (BUET), Dhaka, Bangladesh. The authors also wish to thank the anonymous reviewers and editor for their helpful suggestions and enlightening comments.

References

[1] Rekstad, J., Meir, M., Murtnes, E., Dursun, A., 2015. A comparison of the energy consumption in two passive houses, one with a solar heating system and one with an air–water heat pump. Energy Build. 96, 149–161.
[2] Kabir, E., Kumar, P., Kumar, S., Adelodun, A.A., Kim, K.-H., 2018. Solar energy: Potential and future prospects. Renew. Sustain. Energy Rev. 82, 894–900.
[3] Ahmadi, A., et al., 2021. Recent residential applications of low-temperature solar collector. J. Clean. Prod. 279, 123549.
[4] Jamar, A., Majid, Z.A.A., Azmi, W.H., Norhafana, M., Razak, A.A., 2016. A review of water heating system for solar energy applications. Int. Commun. Heat Mass Transfer 76, 178–187.
[5] Chang, K.-C., Lin, W.-M., Chung, K.-M., 2018. A lesson learned from the long-term subsidy program for solar water heaters in Taiwan. Sustain. Cities Soc. 41, 810–815.
[6] Bait, O., 2019. Exergy, Environ-Economic and economic analyses of a tubular solar water heater assisted solar still. J. Clean. Prod. 212, 630–646.
[7] Gautam, A., Chamoli, S., Kumar, A., Singh, S., 2017. A review on technical improvements, economic feasibility and world scenario of solar water heating system. Renew. Sustain. Energy Rev. 68, 541–562.
[8] Nwaji, G.N., Okoronkwo, C.A., Ogueke, N.V., Anyanwu, E.E., 2019. Hybrid solar water heating/nocturnal radiation cooling system I: A review of the progress, prospects and challenges. Energy Build. 198, 412–430.
[9] Gaonwe, T.P., Kusakana, K., Hohne, P.A., 2022. A review of solar and air-source renewable water heating systems, under the energy management scheme. Energy Rep. 8, 1–10.
[10] Evangelisti, L., De Lieto Vollaro, R., Asdrubali, F., 2019. Latest advances on solar thermal collectors: A comprehensive review. Renew. Sustain. Energy Rev. 114, 109318.
[11] Shemelin, V., Matuska, T., 2022. Unglazed solar thermal collector for building facades. Energy Rep. 8, 605–617.
[12] Chen, W.-L., Chou, H.-M., Yang, Y.-C., 2017. Inverse estimation of the unknown base heat flux in irregular fins made of functionally graded materials. Int. Commun. Heat Mass Transfer 87, 157–163.
[13] Mehmood, A., Waqas, A., Said, Z., Rahman, S.M.A., Akram, M., 2019. Performance evaluation of solar water heating system with heat pipe evacuated tubes provided with natural gas backup. Energy Rep. 5, 1432–1444.
[14] Bamisile, O., Cai, D., Adun, H., Adedeji, M., Dagbasi, M., Dika, F., Huang, Q.i., 2022. A brief review and comparative evaluation of nanofluid application in solar parabolic trough and flat plate collectors. Energy Rep. 8, 156–166.
[15] Seddegh, S., Wang, X., Henderson, A.D., Xing, Z., 2015. Solar domestic hot water systems using latent heat energy storage medium: A review. Renew. Sustain. Energy Rev. 49, 517–533.
[16] Bouhal, T., Agrouaz, Y., Allouhi, A., Kousksou, T., Jamil, A., El Rhafiki, T., Zeraouli, Y., 2017. Impact of load profile and collector technology on the fractional savings of solar domestic water heaters under various climatic conditions. Int. J. Hydrogen Energy 42 (18), 13245–13258.
[17] Tewari, K., Dev, R., 2019. Exergy, environmental and economic analysis of modified domestic solar water heater with glass-to-glass PV module. Energy 170, 1130–1150.
[18] Sabiha, M.A., Saidur, R., Hassani, S., Said, Z., Mekhilef, S., 2015. Energy performance of an evacuated tube solar collector using single walled carbon nanotubes nanofluids. Energ. Conver. Manage. 105, 1377–1388.
[19] Sabiha, M.A., Saidur, R., Mekhilef, S., Mahian, O., 2015. Progress and latest developments of evacuated tube solar collectors. Renew. Sustain. Energy Rev. 51, 1038–1054.
[20] Gill, L., Mac Mahon, J., Ryan, K., 2016. The performance of an evacuated tube solar hot water system in a domestic house throughout a year in a northern maritime climate (Dublin). Sol. Energy 137, 261–272.
[21] Papadimitratos, A., Sobhansarbandi, S., Pozdin, V., Zakhidov, A., Hassanipour, F., 2016. Evacuated tube solar collectors integrated with phase change materials. Sol. Energy 129, 10–19.
[22] Li, X., Dai, Y.J., Li, Y., Wang, R.Z., 2013. Performance investigation on a novel single-pass evacuated tube with a symmetrical compound parabolic concentrator. Sol. Energy 98, 275–289.
[23] Elsheikh, A.H., Sharshir, S.W., Mostafa, M.E., Essa, F.A., Ahmed Ali, M.K., 2018. Applications of nanofluids in solar energy: A review of recent advances. Renew. Sustain. Energy Rev. 82, 3483–3502.
[24] Bait, O., Si–Ameur, M.,, 2016. Enhanced heat and mass transfer in solar stills using nanofluids: A Review. Sol. Energy 170, 694–722.
[25] Bait, O., 2020. Direct and indirect solar–powered desalination processes loaded with nanoparticles: A Review. Sustain. Energy Technol. Assess. 37, 100597.
[26] Karami, M., Akhavan-Bahabadi, M.A., Delfani, S., Raisee, M., 2015. Experimental investigation of CuO nanofluid-based Direct Absorption Solar Collector for residential applications. Renew. Sustain. Energy Rev. 52, 793–801.
[27] Taylor, R.A., Phelan, P.E., Otanicar, T.P., Adrian, R., Prasher, R., 2011. Nanofluid optical property characterization: towards efficient direct absorption solar collectors. Nanoscale Res. Lett. 6 (1).
[28] Li, C., Zhang, B.o., Xie, B., Zhao, X., Chen, J., Chen, Z., Long, Y.i., 2019. Stearic acid/expanded graphite as a composite phase change thermal energy storage material for tankless solar water heater. Sustain. Cities Soc. 44, 458–464.
[29] Thinsurat, K., Bao, H., Ma, Z., Roskilly, A.P., 2019. Performance study of solar photovoltaic-thermal collector for domestic hot water use and thermochemical sorption seasonal storage. Energ. Conver. Manage. 180, 1068–1084.
[30] Salunkhe, P.B., J.k. d,, 2017. Investigations on latent heat storage materials for solar water and space heating applications. J. Storage Mater. 12, 243–260.
[31] Pomianowski, M.Z., et al., 2020. Sustainable and energy-efficient domestic hot water systems: A review. Renew. Sustain. Energy Rev. 128, 109900.
[32] Vengadesan, E., Senthil, R., 2020. A review on recent development of thermal performance enhancement methods of flat plate solar water heater. Sol. Energy 206, 935–961.
[33] Bellos, E., Tzivanidis, C., 2017. Energetic and financial sustainability of solar assisted heat pump heating systems in Europe. Sustain. Cities Soc. 33, 70–84.
[34] Ibrahim, O., Fardoun, F., Younes, R., Louahlia-Gualous, H., 2014. Review of water-heating systems: General selection approach based on energy and environmental aspects. Build. Environ. 72, 259–286.
[35] Ayompe, L.M., Duffy, A., McCormack, S.J., Conlon, M., 2011. Validated TRNSYS model for forced circulation solar water heating systems with flat plate and heat pipe evacuated tube collectors. Appl. Therm. Eng. 31 (8-9), 1536–1542.
[36] Kishor, N., Das, M.K., Narain, A., Prakash Ranjan, V., 2010. Fuzzy model representation of thermosyphon solar water heating system. Sol. Energy 84 (6), 948–955.
[37] Pillai, I.R., Banerjee, R., 2007. Methodology for estimation of potential for solar water heating in a target area. Sol. Energy 81 (2), 162–172.
[38] Hossain, M.S., Saidur, R., Fayaz, H., Rahim, N.A., Islam, M.R., Ahamed, J.U., Rahman, M.M., 2011. Review on solar water heater collector and thermal energy performance of circulating pipe. Renew. Sustain. Energy Rev. 15 (8), 3801–3812.

[39] Liu, S., Afan, H.A., Aldlemy, M.S., Al-Ansari, N., Yaseen, Z.M., 2020. Energy analysis using carbon and metallic oxides-based nanomaterials inside a solar collector. Energy Rep. 6, 1373–1381.
[40] Wang, J., Han, Z., Guan, Z., 2020. Hybrid solar-assisted combined cooling, heating, and power systems: A review. Renew. Sustain. Energy Rev. 133, 110256.
[41] Saghafifar, M., Gabra, S., 2020. A critical overview of solar assisted carbon capture systems: Is solar always the solution? Int. J. Greenhouse Gas Control 92, 102852.
[42] Pinto, R.V., Fiorelli, F.A.S., 2016. Review of the mechanisms responsible for heat transfer enhancement using nanofluids. Appl. Therm. Eng. 108, 720–739.
[43] Singh, R., Lazarus, I.J., Souliotis, M., 2016. Recent developments in integrated collector storage (ICS) solar water heaters: A review. Renew. Sustain. Energy Rev. 54, 270–298.
[44] Santbergen, R., Rindt, C.C.M., Zondag, H.A., van Zolingen, R.J.C., 2010. Detailed analysis of the energy yield of systems with covered sheet-and-tube PVT collectors. Sol. Energy 84 (5), 867–878.
[45] Sarsam, W.S., Kazi, S.N., Badarudin, A., 2015. A review of studies on using nanofluids in flat-plate solar collectors. Sol. Energy 122, 1245–1265.
[46] Saravanan, A., Jaisankar, S., 2019. Heat transfer augmentation techniques in forced flow V-trough solar collector equipped with V-cut and square cut twisted tape. International Journal of Thermal Sciences 140, 59–70.
[47] Wang, D., et al., 2022. Thermal performance analysis of large-scale flat plate solar collectors and regional applicability in China. Energy 238, 121931.
[48] Alwan, N.T., Shcheklein, S.E., Ali, O.M., 2021. Experimental analysis of thermal performance for flat plate solar water collector in the climate conditions of Yekaterinburg, Russia. Mater. Today: Proc. 42, 2076–2083.
[49] Fan, M., Zheng, W., You, S., Zhang, H., Jiang, Y., Wu, Z., 2020. Comparison of different dynamic thermal performance prediction models for the flat-plate solar collector with a new V-corrugated absorber. Sol. Energy 204, 406–418.
[50] Sakhaei, S.A., Valipour, M.S., 2020. Thermal performance analysis of a flat plate solar collector by utilizing helically corrugated risers: An experimental study. Sol. Energy 207, 235–246.
[51] Zhang, D., Tao, H., Wang, M., Sun, Z., Jiang, C., 2017. Numerical simulation investigation on thermal performance of heat pipe flat-plate solar collector. Appl. Therm. Eng. 118, 113–126.
[52] Zheng, W., Yang, L., Zhang, H., You, S., Zhu, C., 2016. Numerical and experimental investigation on a new type of compound parabolic concentrator solar collector. Energ. Conver. Manage. 129, 11–22.
[53] Khamis Mansour, M., 2013. Thermal analysis of novel minichannel-based solar flat-plate collector. Energy 60, 333–343.
[54] Del Col, D., Padovan, A., Bortolato, M., Dai Prè, M., Zambolin, E., 2013. Thermal performance of flat plate solar collectors with sheet-and-tube and roll-bond absorbers. Energy 58, 258–269.
[55] Moss, R., Shire, S., Henshall, P., Arya, F., Eames, P., Hyde, T., 2018. Performance of evacuated flat plate solar thermal collectors. Thermal Sci. Engineering Progress 8, 296–306.
[56] Naik, B.K., Bhowmik, M., Muthukumar, P., 2019. Experimental investigation and numerical modelling on the performance assessments of evacuated U - Tube solar collector systems. Renew. Energy 134, 1344–1361.
[57] Milani, D., Abbas, A., 2016. Multiscale modeling and performance analysis of evacuated tube collectors for solar water heaters using diffuse flat reflector. Renew. Energy 86, 360–374.
[58] Tamuli, B.R., Saikia, S.S., Nath, S., Bhanja, D., 2020. Thermal performance analysis of a co-axial evacuated tube collector with single and two-phase flow consideration under North-eastern India climatic condition. Sol. Energy 196, 107–124.
[59] Mao, C., Li, M., Li, N.a., Shan, M., Yang, X., 2019. Mathematical model development and optimal design of the horizontal all-glass evacuated tube solar collectors integrated with bottom mirror reflectors for solar energy harvesting. Appl. Energy 238, 54–68.
[60] Chopra, K., et al., 2020. Thermal performance of phase change material integrated heat pipe evacuated tube solar collector system: An experimental assessment. Energ. Conver. Manage. 203, 112205.
[61] Yang, J., et al., 2015. A Study on Thermal Performance of a Novel All-Glass Evacuated Tube Solar Collector Manifold Header with an Inserted Tube. Int. J. Photoenergy 2015, 409517.
[62] Chopra, K., et al., 2020. PCM integrated glass in glass tube solar collector for low and medium temperature applications: Thermodynamic & techno-economic approach. Energy 198, 117238.
[63] Liang, R., Ma, L., Zhang, J., Zhao, L., 2013. Performance analysis of a new-design filled-type solar collector with double U-tubes. Energy Build. 57, 220–226.
[64] Nkwetta, D.N., Smyth, M., Haghighat, F., Zacharopoulos, A., Hyde, T., 2013. Experimental performance evaluation and comparative analyses of heat pipe and direct flow augmented solar collectors. Appl. Therm. Eng. 60 (1-2), 225–233.
[65] Terrón-Hernández, M., Peña-Cruz, M., Carrillo, J., Diego-Ayala, U., Flores, V., 2018. Solar Ray Tracing Analysis to Determine Energy Availability in a CPC Designed for Use as a Residential Water Heater. Energies 11 (2), 291.
[66] Gang, P., Guiqiang, L.i., Xi, Z., Jie, J.i., Yuehong, S.u., 2012. Experimental study and exergetic analysis of a CPC-type solar water heater system using higher-temperature circulation in winter. Sol. Energy 86 (5), 1280–1286.
[67] Widyolar, B., Jiang, L., Ferry, J., Winston, R., 2018. Non-tracking East-West XCPC solar thermal collector for 200 celsius applications. Appl. Energy 216, 521–533.
[68] Acuña, A., Velázquez, N., Sauceda, D., Aguilar, A., 2017. Modeling, Construction, and Experimentation of a Compound Parabolic Concentrator with a Concentric Tube as the Absorber. J. Energy Eng. 143 (3).
[69] Parthasarathy, P., Narayanan, S., 2014. Effect of hydrothermal carbonization reaction parameters on. Environ. Prog. Sustain. Energy 33 (3), 676–680.
[70] Satpute, J., Chavan, K., Gulhane, N., 2018. Thermal Performance Investigation of Concentrated Solar Collector Using Novel Aluminum Absorber. Mater. Today:. Proc. 5 (2, Part 1), 4059–4065.
[71] Ambarita, H., Sembiring, P.G., Butarbutar, S., Setiawan, E.Y., 2018. A preliminary test of a flat-plate solar collector of hybrid solar water heater. J. Phys. Conf. Ser. 1116, 032003.
[72] Janjai, S., Esper, A., Mühlbauer, W., 2000. Modelling the performance of a large area plastic solar collector. Renew. Energy 21 (3), 363–376.
[73] Oghogho, I., 2013. Design and construction of a solar water heater based on the thermosyphon principle. J. Fundam. Renew. Energy Appl. 2013 (3), 1–8.
[74] Serale, G., Cascone, Y., Capozzoli, A., Fabrizio, E., Perino, M., 2014. Potentialities of a Low Temperature Solar Heating System Based on Slurry Phase Change Materials (PCS). Energy Procedia 62, 355–363.
[75] Wu, S., Fang, G., Liu, X., 2011. Dynamic discharging characteristics simulation on solar heat storage system with spherical capsules using paraffin as heat storage material. Renew. Energy 36 (4), 1190–1195.
[76] Malvi, C.S., Gupta, A., Gaur, M.K., Crook, R., Dixon-Hardy, D.W., 2017. Experimental investigation of heat removal factor in solar flat plate collector for various flow configurations. Int. J. Green Energy 14 (4), 442–448.
[77] Tripanagnostopoulos, Y., Souliotis, M., Nousia, T., 2000. Solar collectors with colored absorbers. Sol. Energy 68 (4), 343–356.
[78] Kundu, B., 2002. Performance analysis and optimization of absorber plates of different geometry for a flat-plate solar collector: a comparative study. Appl. Therm. Eng. 22 (9), 999–1012.
[79] Shukla, R., Sumathy, K., Erickson, P., Gong, J., 2013. Recent advances in the solar water heating systems: A review. Renew. Sustain. Energy Rev. 19, 173–190.
[80] Xu, G., Chen, W., Deng, S., Zhang, X., Zhao, S., 2015. Performance Evaluation of a Nanofluid-Based Direct Absorption Solar Collector with Parabolic Trough Concentrator. Nanomaterials 5 (4), 2131–2147.
[81] Bait, O., Si-Ameur, M., 2017. Tubular Solar-Energy Collector Integration: Performance Enhancement of Classical Distillation Unit. Energy 141, 818–838.
[82] Kim, Y., Seo, T., 2007. Thermal performances comparisons of the glass evacuated tube solar collectors with shapes of absorber tube. Renew. Energy 32 (5), 772–795.
[83] Olfian, H., Ajarostaghi, S.S.M., Ebrahimnataj, M., 2020. Development on evacuated tube solar collectors: A review of the last decade results of using nanofluids. Sol. Energy 211, 265–282.
[84] Hazami, M., Kooli, S., Naili, N., Farhat, A., 2013. Long-term performances prediction of an evacuated tube solar water heating system used for single-family households under typical Nord-African climate (Tunisia). Sol. Energy 94, 283–298.
[85] Hussein, A.K., 2016. Applications of nanotechnology to improve the performance of solar collectors – Recent advances and overview. Renew. Sustain. Energy Rev. 62, 767–792.
[86] Teles, M.d.P.R., Ismail, K.A.R., Arabkoohsar, A., 2019. A new version of a low concentration evacuated tube solar collector: Optical and thermal investigation. Sol. Energy 180, 324–339.
[87] Pranesh, V., Velraj, R., Christopher, S., Kumaresan, V., 2019. A 50 year review of basic and applied research in compound parabolic concentrating solar thermal collector for domestic and industrial applications. Sol. Energy 187, 293–340.
[88] Jadhav, A.S., Gudekar, A.S., Patil, R.G., Kale, D.M., Panse, S.V., Joshi, J.B., 2013. Performance analysis of a novel and cost effective CPC system. Energ. Conver. Manage. 66, 56–65.
[89] Buttinger, F., Beikircher, T., Pröll, M., Schölkopf, W., 2010. Development of a new flat stationary evacuated CPC-collector for process heat applications. Sol. Energy 84 (7), 1166–1174.
[90] Kalogirou, S.A., 2004. Solar thermal collectors and applications. Prog. Energy Combust. Sci. 30 (3), 231–295.
[91] Kaiyan, H., Hongfei, Z., Tao, T., 2011. A novel multiple curved surfaces compound concentrator. Sol. Energy 85 (3), 523–529.
[92] Souliotis, M., Quinlan, P., Smyth, M., Tripanagnostopoulos, Y., Zacharopoulos, A., Ramirez, M., Yianoulis, P., 2011. Heat retaining integrated collector storage solar water heater with asymmetric CPC reflector. Sol. Energy 85 (10), 2474–2487.
[93] Dai, G.-L., Xia, X.-L., Sun, C., Zhang, H.-C., 2011. Numerical investigation of the solar concentrating characteristics of 3D CPC and CPC-DC. Sol. Energy 85 (11), 2833–2842.
[94] Varghese, J., Samsher, Manjunath, K., 2017. A parametric study of a concentrating integral storage solar water heater for domestic uses. Appl. Therm. Eng. 111, 734–744.
[95] Altuntop, N., Arslan, M., Ozceyhan, V., Kanoglu, M., 2005. Effect of obstacles on thermal stratification in hot water storage tanks. Appl. Therm. Eng. 25 (14-15), 2285–2298.
[96] Gil, A., Medrano, M., Martorell, I., Lázaro, A., Dolado, P., Zalba, B., Cabeza, L.F., 2010. State of the art on high temperature thermal energy storage for power generation. Part 1—Concepts, materials and modellization. Renew. Sustain. Energy Rev. 14 (1), 31–55.
[97] Tian, Y., Zhao, C.Y., 2013. A review of solar collectors and thermal energy storage in solar thermal applications. Appl. Energy 104, 538–553.
[98] Sharif, M.K.A., Al-Abidi, A.A., Mat, S., Sopian, K., Ruslan, M.H., Sulaiman, M.Y., Rosli, M.A.M., 2015. Review of the application of phase change material for heating and domestic hot water systems. Renew. Sustain. Energy Rev. 42, 557–568.

[99] Muneer, T., 1985. Effect of design parameters on performance of built-in-storage solar water heaters. Energ. Conver. Manage. 25 (3), 277–281.
[100] Nam, H., Bai, C., Sim, J., 2014. A study on characteristics of thermal storage tank for varying thermal load in multi-use heat pump water heater. Appl. Therm. Eng. 66 (1), 640–645.
[101] Mohan, G., Venkataraman, M., Gomez-Vidal, J., Coventry, J., 2018. Thermo-economic analysis of high-temperature sensible thermal storage with different ternary eutectic alkali and alkaline earth metal chlorides. Sol. Energy 176, 350–357.
[102] Shah, L.J., Andersen, E., Furbo, S., 2005. Theoretical and experimental investigations of inlet stratifiers for solar storage tanks. Appl. Therm. Eng. 25 (14), 2086–2099.
[103] Shah, L.J., Furbo, S., 2003. Entrance effects in solar storage tanks. Sol. Energy 75 (4), 337–348.
[104] Alizadeh, S., 1999. An experimental and numerical study of thermal stratification in a horizontal cylindrical solar storage tank. Sol. Energy 66 (6), 409–421.
[105] Spur, R., Fiala, D., Nevrala, D., Probert, D., 2006. Performances of modern domestic hot-water stores. Appl. Energy 83 (8), 893–910.
[106] Morrison, G.L., Nasr, A., Behnia, M., Rosengarten, G., 1998. Analysis of horizontal mantle heat exchangers in solar water heating systems. Sol. Energy 64 (1-3), 19–31.
[107] Wang, X., Wang, R., Wu, J., 2005. Experimental investigation of a new-style double-tube heat exchanger for heating crude oil using solar hot water. Appl. Therm. Eng. 25 (11), 1753–1763.
[108] Han, Y.M., Wang, R.Z., Dai, Y.J., 2009. Thermal stratification within the water tank. Renew. Sustain. Energy Rev. 13 (5), 1014–1026.
[109] Tse, K.-K., Chow, T.-T., 2015. Dynamic model and experimental validation of an indirect thermosyphon solar water heater coupled with a parallel circular tube rings type heat exchange coil. Sol. Energy 114, 114–133.
[110] Al-Khaffajy, M., Mossad, R., 2013. Optimization of the heat exchanger in a flat plate indirect heating integrated collector storage solar water heating system. Renew. Energy 57, 413–421.
[111] Shafieian, A., Khiadani, M., Nosrati, A., 2019. Thermal performance of an evacuated tube heat pipe solar water heating system in cold season. Appl. Therm. Eng. 149, 644–657.
[112] Arab, M., Abbas, A., 2013. Model-based design and analysis of heat pipe working fluid for optimal performance in a concentric evacuated tube solar water heater. Sol. Energy 94, 162–176.
[113] Jaisankar, S., Ananth, J., Thulasi, S., Jayasuthakar, S.T., Sheeba, K.N., 2011. A comprehensive review on solar water heaters. Renew. Sustain. Energy Rev. 15 (6), 3045–3050.
[114] Salavati Meibodi, S., Kianifar, A., Niazmand, H., Mahian, O., Wongwises, S., 2015. Experimental investigation on the thermal efficiency and performance characteristics of a flat plate solar collector using SiO2/EG–water nanofluids. Int. Commun. Heat Mass Transfer 65, 71–75.
[115] Azmi, W.H., Sharma, K.V., Mamat, R., Najafi, G., Mohamad, M.S., 2016. The enhancement of effective thermal conductivity and effective dynamic viscosity of nanofluids – A review. Renew. Sustain. Energy Rev. 53, 1046–1058.
[116] Çağlar, A., Yamalı, C., 2012. Performance analysis of a solar-assisted heat pump with an evacuated tubular collector for domestic heating. Energy Build. 54, 22–28.
[117] Xu, K.e., Du, M., Hao, L., Mi, J., Yu, Q., Li, S., 2020. A review of high-temperature selective absorbing coatings for solar thermal applications. J. Materiomics 6 (1), 167–182.
[118] Lizama-Tzec, F.I., Herrera-Zamora, D.M., Arés-Muzio, O., Gómez-Espinoza, V.H., Santos-González, I., Cetina-Dorantes, M., Vega-Poot, A.G., García-Valladares, O., Oskam, G., 2019. Electrodeposition of selective coatings based on black nickel for flat-plate solar water heaters. Sol. Energy 194, 302–310.
[119] Koholé, Y.W., Tchuen, G., 2020. Experimental and numerical investigation of a thermosyphon solar water heater. Int. J. Ambient Energy 41 (4), 384–394.
[120] Ertekin, C., Kulcu, R., F., 2008. Evrendilek *Techno-Economic Analysis of Solar Water Heating Systems inTurkey*. Sensors 8, 1252–1277. https://doi.org/10.3390/s8021252.
[121] El-Sebaii, A.A., Al-Snani, H., 2010. Effect of selective coating on thermal performance of flat plate solar air heaters. Energy 35 (4), 1820–1828.
[122] Sakhrieh, A., Al-Ghandoor, A., 2013. Experimental investigation of the performance of five types of solar collectors. Energ. Conver. Manage. 65, 715–720.
[123] Zhu, Y., Shi, J., Huang, Q., Fang, Y., Wang, L., Xu, G., 2017. A superhydrophobic solar selective absorber used in a flat plate solar collector. RSC Adv. 7 (54), 34125–34130.
[124] Zhang, X.R., Yamaguchi, H., 2008. An experimental study on evacuated tube solar collector using supercritical CO2. Appl. Therm. Eng. 28 (10), 1225–1233.
[125] Gorji, T.B., Ranjbar, A.A., 2017. A review on optical properties and application of nanofluids in direct absorption solar collectors (DASCs). Renew. Sustain. Energy Rev. 72, 10–32.
[126] Saidur, R., Leong, K.Y., Mohammed, H.A., 2011. A review on applications and challenges of nanofluids. Renew. Sustain. Energy Rev. 15 (3), 1646–1668.
[127] Chaji, H., Ajabshirchi, Y., Esmaeilzadeh, E., Zeinali Heris, S., Hedayatizadeh, M., Kahani, M., 2013. Experimental study on thermal efficiency of flat plate solar collector using TiO2/water nanofluid. Mod. Appl. Sci. 7 (10).
[128] Sadri, R., Hosseini, M., Kazi, S.N., Bagheri, S., Abdelrazek, A.H., Ahmadi, G., Zubir, N., Ahmad, R., Abidin, N.I.Z., 2018. A facile, bio-based, novel approach for synthesis of covalently functionalized graphene nanoplatelet nano-coolants toward improved thermo-physical and heat transfer properties. J. Colloid Interface Sci. 509, 140–152.
[129] Zayed, M.E., Zhao, J., Du, Y., Kabeel, A.E., Shalaby, S.M., 2019. Factors affecting the thermal performance of the flat plate solar collector using nanofluids: A review. Sol. Energy 182, 382–396.
[130] An, W., Chen, L.u., Liu, T., Qin, Y., 2018. Enhanced solar distillation by nanofluid-based spectral splitting PV/T technique: Preliminary experiment. Sol. Energy 176, 146–156.
[131] Godson, L., Raja, B., Mohan Lal, D., Wongwises, S., 2010. Enhancement of heat transfer using nanofluids—An overview. Renew. Sustain. Energy Rev. 14 (2), 629–641.
[132] Colangelo, G., Favale, E., de Risi, A., Laforgia, D., 2013. A new solution for reduced sedimentation flat panel solar thermal collector using nanofluids. Appl. Energy 111, 80–93.
[133] Yousefi, T., Veysi, F., Shojaeizadeh, E., Zinadini, S., 2012. An experimental investigation on the effect of Al2O3–H2O nanofluid on the efficiency of flat-plate solar collectors. Renew. Energy 39 (1), 293–298.
[134] Gupta, H.K., Agrawal, G.D., Mathur, J., 2015. An experimental investigation of a low temperature Al2O3-H2O nanofluid based direct absorption solar collector. Sol. Energy 118, 390–396.
[135] Noghrehabadi, A., Hajidavalloo, E., Moravej, M., 2016. Experimental investigation of efficiency of square flat-plate solar collector using SiO2/water nanofluid. Case Studies in Thermal Engineering 8, 378–386.
[136] Said, Z., Sajid, M.H., Alim, M.A., Saidur, R., Rahim, N.A., 2013. Experimental investigation of the thermophysical properties of AL2O3-nanofluid and its effect on a flat plate solar collector. Int. Commun. Heat Mass Transfer 48, 99–107.
[137] Gorji, T.B., Ranjbar, A.A., 2016. A numerical and experimental investigation on the performance of a low-flux direct absorption solar collector (DASC) using graphite, magnetite and silver nanofluids. Sol. Energy 135, 493–505.
[138] Moghadam, A.J., Farzane-Gord, M., Sajadi, M., Hoseyn-Zadeh, M., 2014. Effects of CuO/water nanofluid on the efficiency of a flat-plate solar collector. Exp. Therm Fluid Sci. 58, 9–14.
[139] Mahendran, M., Lee, G.C., Sharma, K.V., Shahrani, A., 2012. Performance of evacuated tube solar collector using water-based titanium oxide nanofluid. Journal of Mechanical Engineering and Sciences 3, 301–310.
[140] He, Q., Wang, S., Zeng, S., Zheng, Z., 2013. Experimental investigation on photothermal properties of nanofluids for direct absorption solar thermal energy systems. Energ. Conver. Manage. 73, 150–157.
[141] Verma, S.K., Tiwari, A.K., Chauhan, D.S., 2017. Experimental evaluation of flat plate solar collector using nanofluids. Energ. Conver. Manage. 134, 103–115.
[142] Lu, L., Liu, Z.-H., Xiao, H.-S., 2011. Thermal performance of an open thermosyphon using nanofluids for high-temperature evacuated tubular solar collectors: Part 1: Indoor experiment. Sol. Energy 85 (2), 379–387.
[143] Delfani, S., Karami, M., Behabadi, M.A.A., 2016. Performance characteristics of a residential-type direct absorption solar collector using MWCNT nanofluid. Renew. Energy 87, 754–764.
[144] Michael, J.J., Iniyan, S., 2015. Performance of copper oxide/water nanofluid in a flat plate solar water heater under natural and forced circulations. Energ. Conver. Manage. 95, 160–169.
[145] Yousefi, T., Veisy, F., Shojaeizadeh, E., Zinadini, S., 2012. An experimental investigation on the effect of MWCNT-H2O nanofluid on the efficiency of flat-plate solar collectors. Exp. Therm Fluid Sci. 39, 207–212.
[146] Said, Z., Sabiha, M.A., Saidur, R., Hepbasli, A., Rahim, N.A., Mekhilef, S., Ward, T. A., 2015. Performance enhancement of a Flat Plate Solar collector using Titanium dioxide nanofluid and Polyethylene Glycol dispersant. J. Clean. Prod. 92, 343–353.
[147] Verma, S.K., Tiwari, A.K., Chauhan, D.S., 2016. Performance augmentation in flat plate solar collector using MgO/water nanofluid. Energ. Conver. Manage. 124, 607–617.
[148] Shojaeizadeh, E., Veysi, F., Kamandi, A., 2015. Exergy efficiency investigation and optimization of an Al2O3–water nanofluid based Flat-plate solar collector. Energy Build. 101, 12–23.
[149] Poongavanam, G.K., Panchabikesan, K., Murugesan, R., Duraisamy, S., Ramalingam, V., 2019. Experimental investigation on heat transfer and pressure drop of MWCNT - Solar glycol based nanofluids in shot peened double pipe heat exchanger. Powder Technol. 345, 815–824.
[150] Mahian, O., Kianifar, A., Sahin, A.Z., Wongwises, S., 2015. Heat Transfer, Pressure Drop, and Entropy Generation in a Solar Collector Using SiO2/Water Nanofluids: Effects of Nanoparticle Size and pH. J. Heat Transfer 137 (6).
[151] Ghaderian, J., Sidik, N.A.C., 2017. An experimental investigation on the effect of Al2O3/distilled water nanofluid on the energy efficiency of evacuated tube solar collector. Int. J. Heat Mass Transf. 108, 972–987.
[152] Faizal, M., Saidur, R., Mekhilef, S., Alim, M.A., 2013. Energy, economic and environmental analysis of metal oxides nanofluid for flat-plate solar collector. Energ. Conver. Manage. 76, 162–168.
[153] Ghaderian, J., Sidik, N.A.C., Kasaeian, A., Ghaderian, S., Okhovat, A., Pakzadeh, A., Samion, S., Yahya, W.J., 2017. Performance of copper oxide/distilled water nanofluid in evacuated tube solar collector (ETSC) water heater with internal coil under thermosyphon system circulations. Appl. Therm. Eng. 121, 520–536.
[154] Tong, Y., Kim, J., Cho, H., 2015. Effects of thermal performance of enclosed-type evacuated U-tube solar collector with multi-walled carbon nanotube/water nanofluid. Renew. Energy 83, 463–473.
[155] Vakili, M., Hosseinalipour, S.M., Delfani, S., Khosrojerdi, S., Karami, M., 2016. Experimental investigation of graphene nanoplatelets nanofluid-based volumetric solar collector for domestic hot water systems. Sol. Energy 131, 119–130.
[156] Nasrin, R., Alim, M., 2015. Thermal performance of nanofluid filled solar flat plate collector. Int. J. Heat Technol. 33 (2), 17–24.

[157] Gorji, T.B., Ranjbar, A.A., 2017. Thermal and exergy optimization of a nanofluid-based direct absorption solar collector. Renew. Energy 106, 274–287.
[158] He, Q., Zeng, S., Wang, S., 2015. Experimental investigation on the efficiency of flat-plate solar collectors with nanofluids. Appl. Therm. Eng. 88, 165–171.
[159] Eidan, A.A., AlSahlani, A., Ahmed, A.Q., Al-fahham, M., Jalil, J.M., 2018. Improving the performance of heat pipe-evacuated tube solar collector experimentally by using Al2O3 and CuO/acetone nanofluids. Sol. Energy 173, 780–788.
[160] Borode, A., Ahmed, N., Olubambi, P., 2019. A review of solar collectors using carbon-based nanofluids. J. Clean. Prod. 241, 118311.
[161] Taylor, R.A., et al., Applicability of nanofluids in high flux solar collectors. *Journal of Renewable and Sustainable Energy*, 2011. 3(2): p. 023104.
[162] Salman, M.S., Znad, H., Hasan, M.N., Hasan, M.M., 2021. Optimization of innovative composite sensor for Pb(II) detection and capturing from water samples. Microchem. J. 160, 105765.
[163] Hasan, M.M., Kubra, K.T., Hasan, M.N., Salman, M.S., Sheikh, M.C., Rehan, A.I., Rasee, A.I., Waliullah, R.M., Islam, M.S., Khandaker, S., Islam, A., Hossain, M.S., Alsukaibi, A.K.D., Alshammari, H.M., 2023. Sustainable ligand-modified based composite material for the selective and effective cadmium(II) capturing from wastewater. J. Mol. Liq. 371, 121125.
[164] Hasan, M.N., Salman, M.S., Islam, A., Znad, H., Hasan, M.M., 2021. Sustainable composite sensor material for optical cadmium(II) monitoring and capturing from wastewater. Microchem. J. 161, 105800.
[165] Hasan, M.N., Salman, M.S., Hasan, M.M., Kubra, K.T., Sheikh, M.C., Rehan, A.I., Rasee, A.I., Waliullah, R.M., Hossain, M.S., Islam, A., Khandaker, S., Alsukaibi, A. K.D., Alshammari, H.M., 2023. Assessing sustainable Lutetium(III) ions adsorption and recovery using novel composite hybrid nanomaterials. J. Mol. Struct. 1276, 134795.
[166] Kubra, K.T., Salman, M.S., Hasan, M.N., 2021. Enhanced toxic dye removal from wastewater using biodegradable polymeric natural adsorbent. J. Mol. Liq. 328, 115468.
[167] Salman, M.S., Hasan, M.N., Hasan, M.M., Kubra, K.T., Sheikh, M.C., Rehan, A.I., Waliullah, R.M., Rasee, A.I., Hossain, M.S., Alsukaibi, A.K.D., Alshammari, H.M., 2023. Improving copper(II) ion detection and adsorption from wastewater by the ligand-functionalized composite adsorbent. J. Mol. Struct. 1282, 135259.
[168] Shahat, A., Kubra, K.T., Salman, M.S., Hasan, M.N., Hasan, M.M., 2021. Novel solid-state sensor material for efficient cadmium(II) detection and capturing from wastewater. Microchem. J. 164, 105967.
[169] Kubra, K.T., Hasan, M.M., Hasan, M.N., Salman, M.S., Khaleque, M.A., Sheikh, M. C., Rehan, A.I., Rasee, A.I., Waliullah, R.M., Hossain, M.S., Alsukaibi, A.K.D., Alshammari, H.M., 2023. The heavy lanthanide of Thulium(III) separation and recovery using specific ligand-based facial composite adsorbent. Colloid. Surface. A 667, 131415.
[170] Rastogi, R., Kaushal, R., Tripathi, S.K., Sharma, A.L., Kaur, I., Bharadwaj, L.M., 2008. Comparative study of carbon nanotube dispersion using surfactants. J. Colloid Interface Sci. 328 (2), 421–428.
[171] Bioucas, F.E.B., Vieira, S.I.C., Lourenço, M.J.V., Santos, F.J.V., Nieto de Castro, C. A., 2018. Performance of heat transfer fluids with nanographene in a pilot solar collector. Sol. Energy 172, 171–176.
[172] Jamal-Abad, M.T., Zamzamian, A., Imani, E., Mansouri, M., 2013. Experimental Study of the Performance of a Flat-Plate Collector Using Cu–Water Nanofluid. J. Thermophys Heat Transfer 27 (4), 756–760.
[173] Liu, Z.-H., Hu, R.-L., Lu, L., Zhao, F., Xiao, H.-S., 2013. Thermal performance of an open thermosyphon using nanofluid for evacuated tubular high temperature air solar collector. Energ. Conver. Manage. 73, 135–143.
[174] Kim, H., Ham, J., Park, C., Cho, H., 2016. Theoretical investigation of the efficiency of a U-tube solar collector using various nanofluids. Energy 94, 497–507.
[175] Iranmanesh, S., Ong, H.C., Ang, B.C., Sadeghinezhad, E., Esmaeilzadeh, A., Mehrali, M., 2017. Thermal performance enhancement of an evacuated tube solar collector using graphene nanoplatelets nanofluid. J. Clean. Prod. 162, 121–129.
[176] Hussain, H.A., Jawad, Q., Sultan, K.F., 2015. Experimental analysis on thermal efficiency of evacuated tube solar collector by using nanofluids. International Journal of Sustainable and Green Energy 4 (3–1), 19–28.
[177] Kumar, A., Sharma, M., Thakur, P., Thakur, V.K., Rahatekar, S.S., Kumar, R., 2020. A review on exergy analysis of solar parabolic collectors. Sol. Energy 197, 411–432.
[178] Gorjian, S., et al., 2020. A review on recent advancements in performance enhancement techniques for low-temperature solar collectors. Energ. Conver. Manage. 222, 113246.
[179] Salman, M.S., Hasan, M.N., Kubra, K.T., Hasan, M.M., 2021. Optical detection and recovery of Yb(III) from waste sample using novel sensor ensemble nanomaterials. Microchem. J. 162, 105868.
[180] Hasan, M.N., Hasan, M.M., Salman, M.S., Sheikh, M.C., Kubra, K.T., Islam, M.S., Marwani, H.M., Islam, A., Khaleque, M.A., Waliullah, R.M., Hossain, M.S., Rasee, A.I., Rehan, A.I., 2023. Green and robust adsorption and recovery of Europium(III) with a mechanism using hybrid donor conjugate materials. Sep. Purif. Technol. 319, 124088.
[181] Kubra, K.T., Salman, M.S., Znad, H., Hasan, M.N., 2021. Efficient encapsulation of toxic dye from wastewater using biodegradable polymeric adsorbent. J. Mol. Liq. 329, 115541.
[182] Salman, M.S., Sheikh, M.C., Hasan, M.M., Hasan, M.N., Kubra, K.T., Rehan, A.I., Rasee, A.I., Waliullah, R.M., Hossain, M.S., Khaleque, M.A., Alsukaibi, A.K.D., Alshammari, H.M., 2023. Chitosan-coated cotton fiber composite for efficient toxic dye encapsulation from aqueous media. Appl. Surf. Sci. 622, 157008.
[183] Al-Hazmi, G.H., Refat, M.S., Alshammari, K.F., Kubra, K.T., Shahat, A., 2023. Efficient toxic doxorubicin hydrochloride removal from aqueous solutions using facial alumina nanorods. J. Mol. Struct. 1272, 134187.
[184] Hasan, M.M., Salman, M.S., Hasan, M.N., Rehan, A.I., Rasee, A.I., Waliullah, R.M., Hossain, M.S., Kubra, K.T., Sheikh, M.C., Khaleque, M.A., Marwani, H.M., Islam, A., 2023. Facial conjugate adsorbent for sustainable Pb(II) ion monitoring and removal from contaminated water. Colloid. Surface. A 673, 131794.
[185] Shahat, A., Kubra, K.T., El-marghany, A., 2023. Equilibrium, thermodynamic and kinetic modeling of triclosan adsorption on mesoporous carbon nanosphere: Optimization using Box-Behnken design. J. Mol. Liq. 383, 122166.
[186] Rehan, A.I., Rasee, A.I., Waliullah, R.M., Hossain, M.S., Kubra, K.T., Salman, M.S., Hasan, M.M., Hasan, M.N., Sheikh, M.C., Marwani, H.M., Khaleque, M.A., Islam, A., 2023. Improving toxic dye removal and remediation using novel nanocomposite fibrous adsorbent. Colloids Surf. A 673, 131859.
[187] Rasee, A.I., Awual, E., Rehan, A.I., Hossain, M.S., Waliullah, R.M., Kubra, K.T., Sheikh, M.C., Salman, M.S., Hasan, M.N., Hasan, M.M., Marwani, H.M., Islam, A., Khaleque, M.A., Awual, M.R., 2023. Efficient separation, adsorption, and recovery of Samarium(III) ions using novel ligand-based composite adsorbent. Surf. Interfaces 41, 103276.
[188] Rahman, T.U., Roy, H., Fariha, A., Shoronika, A.Z., Al-Mamun, M.R., Islam, S.Z., Islam, M.S., Marwani, H.M., Islam, A., Alsukaibi, A.K.D., Rahman, M.M., 2023. Progress in plasma-based doping semiconductor photocatalysts for efficient pollutant remediation and hydrogen generation. Sep. Purif. Technol. 320, 124141.
[189] Roy, H., Rahman, T.U., Khan, M.A.J.R., Al-Mamun, M.R., Islam, S.Z., Khaleque, M.A., Hossain, M.I., Khan, M.Z.H., Islam, M.S., Marwani, H.M., Islam, A., Hasan, M.M., Awual, M.R., 2023. Toxic dye removal, remediation, and mechanism with doped SnO_2-based nanocomposite photocatalysts: A critical review. J. Water Process Eng. 54, 104069.
[190] Kasaeian, A., Daviran, S., Azarian, R.D., Rashidi, A., 2015. Performance evaluation and nanofluid using capability study of a solar parabolic trough collector. Energ. Conver. Manage. 89, 368–375.
[191] Ghasemi, S.E. and A.G.R. MEHDIZADEH, Numerical analysis of performance of solar parabolic trough collector with Cu-water nanofluid. 2014.
[192] Wang, Y., Xu, J., Liu, Q., Chen, Y., Liu, H., 2016. Performance analysis of a parabolic trough solar collector using Al2O3/synthetic oil nanofluid. Appl. Therm. Eng. 107, 469–478.
[193] Waliullah, R.M., Rehan, A.I., Awual, M.E., Rasee, A.I., Sheikh, M.C., Salman, M.S., Hossain, M.S., Hasan, M.M., Kubra, K.T., Hasan, M.N., Marwani, H.M., Islam, A., Rahman, M.M., Khaleque, M.A., Awual, M.R., 2023. Optimization of toxic dye removal from contaminated water using chitosan-grafted novel nanocomposite adsorbent. J. Mol. Liq. 388, 122763.
[194] Sheikh, M.C., Hasan, M.M., Hasan, M.N., Salman, M.S., Kubra, K.T., Awual, M.E., Waliullah, R.M., Rasee, A.I., Rehan, A.I., Hossain, M.S., Marwani, H.M., Islam, A., Khaleque, M.A., Awual, M.R., 2023. Toxic cadmium(II) monitoring and removal from aqueous solution using ligand-based facial composite adsorbent. J. Mol. Liq. 389, 122854.
[195] Rahman, T.U., Roy, H., Shoronika, A.Z., Fariha, A., Hasan, M., Islam, M.S., Marwani, H.M., Islam, A., Hasan, M.M., Alsukaibi, A.K.D., Rahman, M.M., Awual, M.R., 2023. Sustainable toxic dye removal and degradation from wastewater using novel chitosan-modified TiO_2 and ZnO nanocomposites. J. Mol. Liq. 388, 122764.
[196] Khan, M.S., Abid, M., Ratlamwala, T.A.H., 2019. Energy, Exergy and Economic Feasibility Analyses of a 60 MW Conventional Steam Power Plant Integrated with Parabolic Trough Solar Collectors Using Nanofluids. Iranian Journal of Science and Technology, Transactions of Mechanical Engineering 43 (1), 193–209.
[197] Khakrah, H., Shamloo, A., Kazemzadeh Hannani, S., 2018. Exergy analysis of parabolic trough solar collectors using Al2O3/synthetic oil nanofluid. Sol. Energy 173, 1236–1247.
[198] Hordy, N., et al., 2015. A Stable Carbon Nanotube Nanofluid for Latent Heat-Driven Volumetric Absorption Solar Heating Applications. J. Nanomater. 2015, 850217.
[199] Luo, Z., Wang, C., Wei, W., Xiao, G., Ni, M., 2014. Performance improvement of a nanofluid solar collector based on direct absorption collection (DAC) concepts. Int. J. Heat Mass Transf. 75, 262–271.
[200] Beicker, C.L.L., Amjad, M., Bandarra Filho, E.P., Wen, D., 2018. Experimental study of photothermal conversion using gold/water and MWCNT/water nanofluids. Sol. Energy Mater. Sol. Cells 188, 51–65.
[201] Xu, X., Xu, C., Liu, J., Fang, X., Zhang, Z., 2019. A direct absorption solar collector based on a water-ethylene glycol based nanofluid with anti-freeze property and excellent dispersion stability. Renew. Energy 133, 760–769.
[202] Sharma, N., 2021. Public perceptions towards adoption of residential solar water heaters in USA: A case study of Phoenicians in Arizona. J. Clean. Prod. 320, 128891.